International Journal of Adhesion & Adhesives 31 (2011) 248–264

Contents lists available at ScienceDirect

International Journal of Adhesion & Adhesives

journal homepage: www.elsevier.com/locate/ijadhadh

A review of finite element analysis of adhesively bonded joints

Xiaocong He*

Innovative Manufacturing Research Centre, Kunming University of Science and Technology, Kunming 650093, China

ARTICLE INFO

Article history:
Accepted 26 January 2011
Available online 24 February 2011

Keywords:
Adhesive bonding
Joint design
Finite element stress analysis
Fracture mechanics
Dynamic mechanical analysis

ABSTRACT

The need to design lightweight structures and the increased use of lightweight materials in industrial fields, have led to wide use of adhesive bonding. Recent work relating to finite element analysis of adhesively bonded joints is reviewed in this paper, in terms of static loading analysis, environmental behaviors, fatigue loading analysis and dynamic characteristics of the adhesively bonded joints. It is concluded that the finite element analysis of adhesively bonded joints will help future applications of adhesive bonding by allowing system parameters to be selected to give as large a process window as possible for successful joint manufacture. This will allow many different designs to be simulated in order to perform a selection of different designs before testing, which would currently take too long to perform or be prohibitively expensive in practice.

1. Introduction

Due to the increasing demand for energy-efficient vehicles, there is an increasing need to design lightweight structures such as aircraft and vehicle body frames. Because of this factor and due to the increased use of lightweight materials, sheet material joining techniques have been developed rapidly in recent years for joining advanced lightweight materials that are dissimilar, coated and hard to weld [1,2].

As a traditional joining method, adhesive bonding has been used for many centuries. However, it is only in the last seventy years that the science and technology of adhesive bonding has really progressed significantly [3–5]. There is considerable use of adhesive bonding in different industrial fields. Up until 2009, for example, the market demand for automobile adhesives was viewed as increasing very fast and the average per-vehicle consumption of adhesives/sealants was around 20 kg. The structural automotive adhesives would have an average annual growth rate of greater than 7% over the next five years. In the aerospace industry, more and more adhesives have been used in the construction of the aircraft culminating in the Boeing 787 and the Airbus A350 both of which contain more than 50% bonded structure [6]. This widespread use of adhesive bonding is due to ease of application, time and cost savings, high corrosion and fatigue resistance, crack retardance and good damping characteristics [7–9].

Fig. 1 shows some typical classifications of adhesively bonded joints, which are commonly found in current engineering practice. The spew can be considered as the result of the adhesive squeezed out of the lap region at the moment of the joint manufacture. The mechanical behavior of an adhesively bonded joint can be obtained by closed-form equations or experiments. For a fast and easy answer, a closed-form analysis is appropriate. In Volkersen's shear-lag analysis [10], it was assumed that the adhesive deforms only in shear, while the adherend deforms only in tension. The consequences of the rotation of the adherends were first taken into account by Goland and Reissner [11]. They derived equations to evaluate the shearing and normal stresses in the bond layer as well as those in the jointed plates, assuming that the peel and shear stresses were constants across the adhesive thickness. In Cornell's work [12], a variation and extension of Goland and Reissner's method was presented for determining the stresses in adhesive lap-joints. He assumes that the two lap-joint plates act like simple beam and the more elastic adhesive layer is an infinite number of shear and tension springs. Hart-Smith has produced an enormous amount of work on continuum mechanics of adhesive joints, for example [13–15]. His method is a development of the shear-lag analysis of Volkersen and the two theories of Goland and Reissner. The design philosophy behind Hart-Smith's work is that the adhesive should not be the weak link. Thus, if peel stresses are likely to occur, they should be alleviated by tapering the adherends (scarfing) or by locally thickening the adhesive layer.

The mechanical behavior of adhesively bonded joints is not only influenced by the geometry of the joints but also by different boundary conditions. The increasing complex joint geometry and its three-dimensional nature combine to increase the difficulty of obtaining an overall system of governing equations for predicting the mechanical properties of the adhesively bonded joints. In addition, material non-linearity due to plastic behavior is difficult

* Tel.: +86 871 5170912; fax: +86 871 5194243.
E-mail address: hhxxcc@yahoo.co.uk

0143-7496/$ - see front matter © 2011 Elsevier Ltd. All rights reserved.
doi:10.1016/j.ijadhadh.2011.01.006

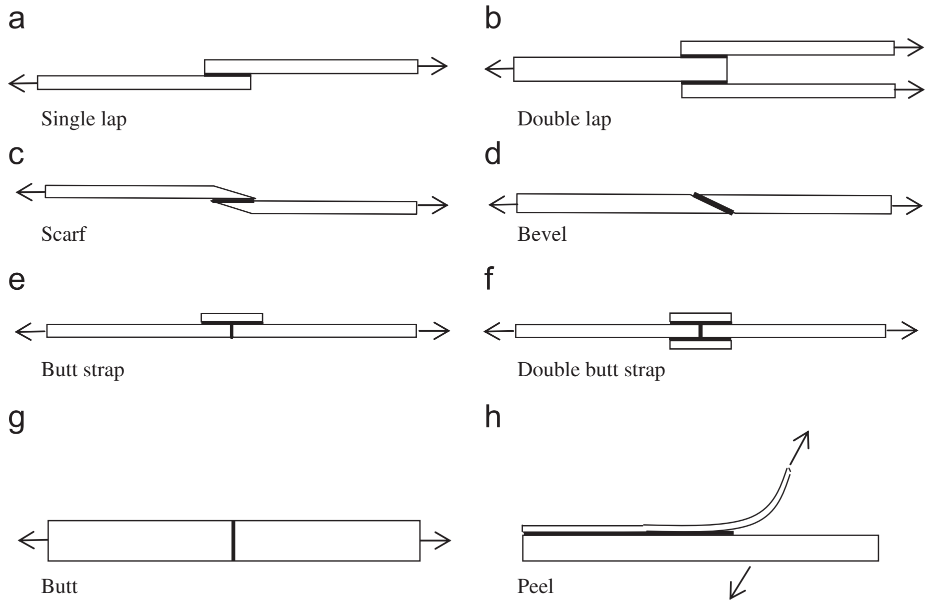

Fig. 1. Some common engineering adhesive joints.

to incorporate because the analysis becomes very complex in the mathematical formulation. The experiments are often time consuming and costly. To overcome these problems, the finite element analysis (FEA) is frequently used since 1970s.

The FEA has the great advantage that the mechanical properties in an adhesively bonded joint of almost any geometrical shape under various load conditions can be determined. In the case of FEA of adhesively bonded joints, however, the thickness of adhesive layer is much smaller than that of the adherends. The finite element mesh must accommodate both the small dimension of the adhesive layer and the larger dimension of the remainder of the whole model. Moreover, the failures of adhesively bonded joints usually occur inside the adhesive layer. It is essential to model the adhesive layer by a finite element mesh which is smaller than the adhesive layer thickness. The result is that the finite element mesh must be several orders of magnitude more refined in a very small region than is needed in the rest of the joint. Thus the number of degrees of freedom in an adhesively bonded joint is rather high. It is also important that a smooth transition between the adherends and adhesive be provided. Fig. 2 shows an example of smooth transition between the adherends and adhesive [16].

It is of course important to build the finite element model with a limited number of elements and nodes to save computer time. The simplified models, however, have sometimes restricted the full view and the accuracy of the results. The application of the explicit FE-codes in FEA of adhesively bonded joints has increased significantly in recent years. Using the explicit FE-codes, the equation of motion of each degree of freedom is solved individually. This allows for very large models such as detailed craft structures, which even consist of over one million degrees of freedom, to be simulated within a reasonable execution time. The limit on the degrees of freedom is due to limits in computer memory capacity and on the need to keep the solution time reasonable.

In the area of FEA of adhesive bonding, the work by Adams et al. from the University of Bristol is regarded as a seminal work [e.g., 17–27]. Adams et al. took the lead to carrying out the FEA for different adhesively bonded joints such as lap joints [17], tubular lap joints [18], butt joints [19], bevel and scarf joints [20].

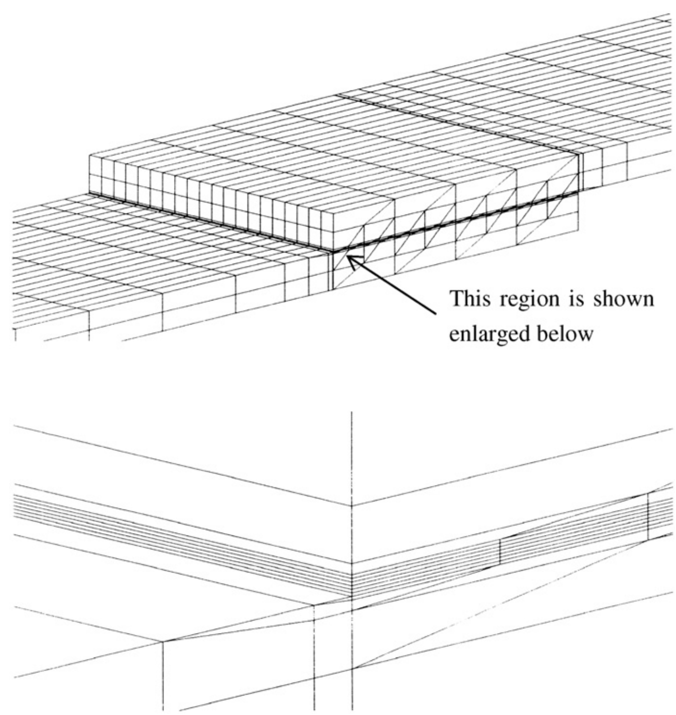

Fig. 2. An example of smooth transition between adherends and adhesive [16].

They also introduced elasto-plastic and non-linear FEA into adhesive bonding [21,24]. Their work has led the development of FEA in adhesive bonding.

A considerable amount of FEA has been carried out on different types of adhesively bonded joints over the years. Mackerle [28,29] gives bibliographical reviews of the finite element methods applied to the analysis and simulation of adhesive bonding. Baldan [30,31] gives very comprehensive reviews on the adhesively bonded joints in different materials. Banea and da Silva [32] give a very comprehensive review on the adhesively bonded joints in composite materials.

In recent years, some exciting developments of FEA of adhesive bonding have been accompanied by scientific research such as at Erciyes University [e.g., 33–37], University of Porto [e.g., 38–45], Hiroshima University [e.g., 46–50], Dalhousie University [e.g., 51–55], University of Surrey [e.g., 56–60] and China Three Gorges University [e.g., 61–65], etc. For having a knowledge of the recent progress in FEA of the adhesive bonding, published work in recent years relating to the FEA of the adhesively bonded joints is reviewed in this paper, in terms of static loading analysis, environmental behaviors, fatigue loading analysis, dynamic characteristics of the adhesively bonded joints.

2. Static loading analysis

Adhesively bonded joints occurring in practice are designed to carry a given set of loads. The subsequent loads on the adhesive are then a function of the geometry of the joint. A common type of mechanical loading encountered by adhesively bonded joints such as in civil engineering is static loading. In addition, static analysis of adhesively bonded joints will provide a basis for further fatigue, dynamic analyses of the joints.

2.1. Stress distribution

The adhesively bonded joints should be designed to minimize stress concentrations. Some stresses, such as peel and cleavage, should also be minimized since these stresses are ultimately responsible for the failure of the joints. Static stress analyses have been carried out for various joint configurations, different material properties and different loading conditions.

2.1.1. Single-lap joint

In order to determine the physical nature of stress distribution in adhesively bonded joints, the single-lap joints (SLJs) have been investigated by many researchers owing to its simple and convenient test geometry. The lap-joint problem is three-dimensional although it has a simple geometry. The stress behavior of the SLJs is rather complex since bending is induced during the deformation. It is found that the highest stresses and strain in the SLJs occur in regions at the edge of the overlap. The use of the FEA enables the distributions in the critical regions to be predicted with reasonable accuracy.

Based on a two-dimensional elasticity theory that both includes the complete stress–strain and the complete strain–displacement relationships for the adhesive and adherends, a general two-dimensional (2D) theoretical approach capable of providing an explicit closed-form solution was developed by Zhao and Lu [66] for the calculation of elastic stresses in SLJs. The calibration of the approach was verified by comparing it with the previously theoretical solutions, and the 2D geometrically nonlinear finite element models with the rotation and non-rotation boundary conditions.

He and Oyadiji [67] investigated the influence on the stresses of the SLJs using adhesives of different characteristics, which encompass the entire spectrum of viscoelastic behavior. The maximum stress ratio was used to determine maximum values of Young's modulus required in order that the static stresses of an adhesively bonded cantilevered beam will not be more than a given value of that of the equivalent homogeneous structure, that is a geometrically similar beam but without a joint. In another paper, the stress distribution along the whole SLJs was investigated by the same authors [68]. The FEA results indicated that there are stress discontinuities existing at the lower interface and the upper interface for longitudinal stress and peel stress components.

Using the FEA, Haghani et al. [69] carried out a parametric study to investigate the effect of tapering length and the material properties of joint constituents on stress distribution in adhesive joints. The results indicated that the effect of tapering on stress distribution is highly dependent on the stiffness of the laminate and the adhesive used in the joint. Reverse tapering was found to have more favorable effects on stress reduction in comparison to normal tapering.

Fessel et al. [70] compared the stress distribution of the 'reverse-bent' and the 'wavy joint', with the stresses of the traditional lap–shear joint. The joint strength of 'reverse-bent' joints was found to be up to 40% higher compared to flat joints using various substrate materials, adhesives and overlap lengths. However, it was shown that the joint strength is strongly dependent on the yield point of the metallic substrates. The lap–shear joints failed mostly due to the bending and subsequently yielding of the substrates, whereas the reverse-bent joints failed predominantly in shear or due to lateral straining of the substrates away from the overlap.

Zhao et al. [71] proposed a new method of determining bending moments at the overlap ends of SLJs. Examples showed that the method is better than those of the Goland and Reissner and of the Hart-Smith for overlaps up to 25 mm long. Experimental and numerical analysis of SLJs were also carried out by Grant et al. [72]. Various parameters were investigated such as the overlap length, the bondline thickness and the spew fillet. The major finding was that three-point bending and tension loading are very similar in the way in which they affect the adhesive while the four-point bend test does not cause failure because the steel yields before the joint fails. Diaz et al. [73] carried out a benchmark investigation of 3D finite element models of carbon fiber-reinforced polymer (CFRP) SLJs. All the simulations were conducted with 3D meshes and geometrical non-linearity was considered.

The influence of the height and angle of the inner chamfer near the ends of the adherends and the elastic modulus of several adhesives on the stress distribution in SLJs was investigated by You et al. [74] using both the elasto-plastic FEA and experimental methods. In another paper [75], You et al. investigated the effects of preformed angle on the stress distribution in the mid-bondline and the ultimate load of the adhesively bonded steel SLJs. The results from the numerical simulation showed that all the peak stresses in the mid-bondline of the adhesively bonded SLJ were reduced as the preformed deflection angle was increased from 0°

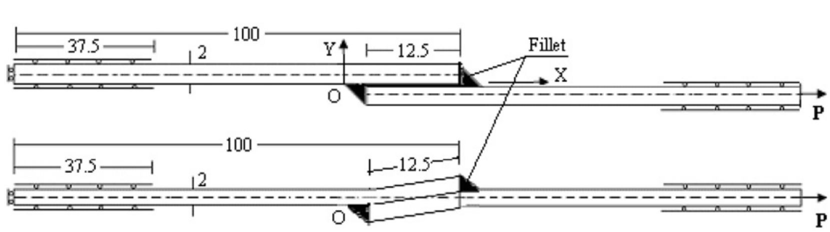

Fig. 3. Sketch of a standard SLJ and a SLJ with a 10° preformed angle [75].

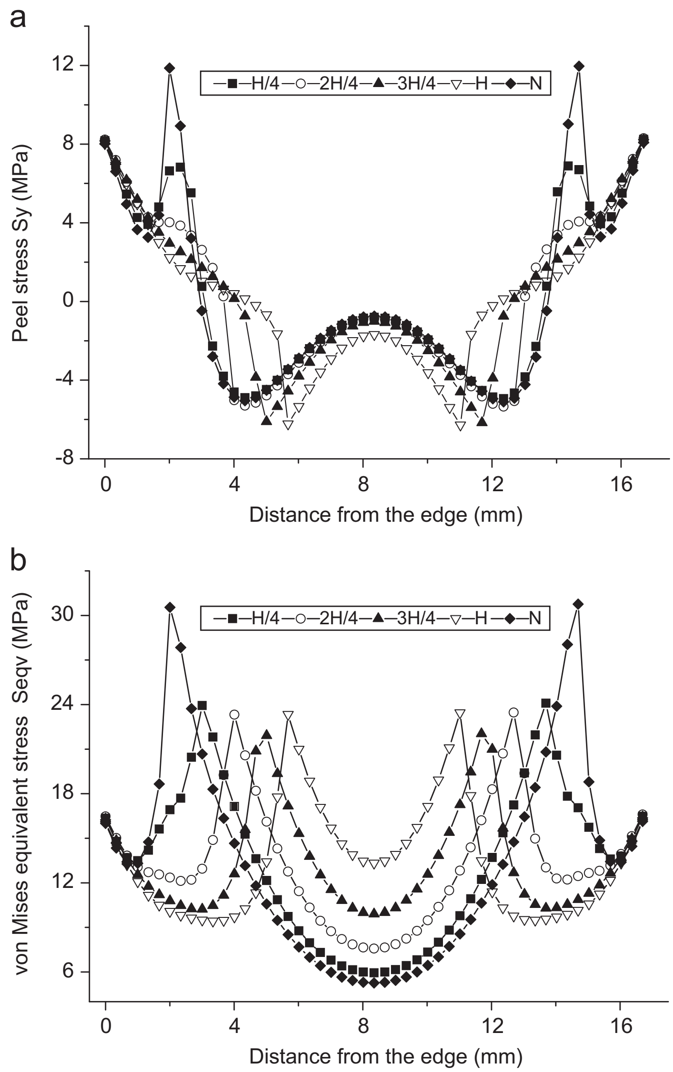

Fig. 4. Effects of the chamfer height on stress distribution in the joint (redrawn from [74]).

to 15°. Fig. 3 shows a standard SLJ and a SLJ with a preformed angle. Fig. 4 shows the effect of the chamfer height on the stress distribution of a SLJ.

Pereira et al. [76] studied the effect of geometrical and manufacturing parameters on the strength of adhesively bonded SLJs with the aim of optimizing shear strength. The surface treatments process using sodium dichromate-sulphuric acid etch (CSA) and abrasive polishing (AP) resulted in improved joint shear strength when compared to acetone cleaning (SW), caustic etch (CE) and Tucker's reagent etch (TR). The FEA was developed to explain the effect of the geometrical parameters on rotation angle, stress and strain fields and failure load. Rudawska's paper [77] compared experimental data with FEA results for adhesive joints made of titanium sheet, aluminum sheet and aramidepoxy composite using a number of different joint assemblies.

Kumar and Pandey's study [78] presented the 2D and 3D non-linear (geometric and material) FEAs of adhesively bonded SLJ having modulus-graded bondline under monotonic loading conditions. The adhesives were modeled as an elasto-plastic multi-linear material, while the substrates were regarded as both linear elastic and bi-linear elasto-plastic material. 3D analysis results reveal the existence of complex multi-axial stress/strain state at the ends of the overlap in the bondline which cannot be observed in 2D plane strain analysis.

2.1.2. Other types of adhesive joints

As mentioned above, though the most widely used adhesively bonded joint type is the SLJ, many other types of joints are designed to decrease the peel stresses. Such as the double lap, the scarf, the bevel, the butt strap, the double butt strap and the butt, etc. Linear and non-linear FEA have been carried out on different types of adhesively bonded joints, and the adhesive effective stresses and strains have been evaluated.

Llopart et al. [79] investigated the influence of imperfect bonding, owing to partial lack of adhesive, on the strength of composite non-crimp fabric (NCF) double-lap shear (DLS) joints experimentally and numerically. A mesomechanical model based on the FEA method and the (homogenized) progressive failure analysis method was developed. Numerical simulations of failure initiation and progression at the NCF joint and the adhesive indicated that it is possible to predict the strength and failure mechanisms of the imperfect bonded DLS joints.

In Ruiz et al.'s work [80], strain distributions within adhesively bonded double-lap shear joints under tensile load were investigated experimentally using the complementary experimental techniques of neutron diffraction (ND) and moire interferometry (MI). FEA was used to verify the resulting comprehensive datasets obtained from both aluminum and steel joints. In a similar topic, Jumbo et al. [81] investigated the residual and mechanical strains in aluminum/aluminum (Al/Al) and aluminum/carbon fiber-reinforced polymer (Al/CFRP) adhesively bonded double-lap joints. Residual strains were measured inside the adherends by means of neutron diffraction (ND) and modeled using FEA. Although considerable scatter was seen in the ND results, the measured and predicted trends showed similar behavior and were of comparable magnitude.

You et al. [82] studied the effect of the gap, as well as its length, on the stress distribution in both the mid-bondline and the adherend near the interface along the lap zone of adhesively bonded aluminum double-lap joint. The results from the FEA simulation showed that the effect of the gap length on the ultimate load of the joint was small as the gap length was increased. Ascione and Mancusi [83] carried out an axial/bending coupled analysis for fiber-reinforced polymer (FRP) adhesive double-lap joints. The paper took into account the coupling effects between shear/flexure and extensional equilibrium problems. Chataigner et al. [84] introduced an analytical procedure based on the well-known Shear Lag theory of Volkersen, but allowing to take into account a multilinear mechanical behavior of the adhesive in order to determine an average shear stress profile along the bonded joint. Different parameters of the joint were varied so that it is possible to check qualitative expectations, and define a quantitative failure prediction parameter. The shear stress profiles obtained using the described analytical procedures were compared to the FEA results and good agreement was found between both approaches.

In a recent study, Apalak [85] investigated the 3D elastic flexural stresses in an adhesively bonded functionally graded double containment cantilever joint. The mechanical properties of the through-thickness graded region between a ceramic (Al_2O_3) top layer and a metal (Ni) bottom layer were defined based on a power law distribution and modeled with a layered 3D finite element. The artificial neural network (ANN) combined with FEA indicated that the compositional gradient exponent, the support length and the plate thickness affected considerably the elastic strain energy using whereas the adhesive thickness has minor effect.

In Chaves et al.'s paper [86], FEA was used to optimize the initial geometry of the adhesively bonded T-joints for assessing the applicability of adhesives to connect a transom to a polyvinyl chloride window frame. Experiments and FEA were carried out by

Grant et al. [87] for T-peel joints. Various parameters, such as the bondline thickness and adherend radius, were investigated. It was found that contrary to the case of lap joints, there are no stress concentrations around the fillet area and, then it is possible to use the maximum uniaxial tensile stress as a failure criterion for these joints. Hosseinzadeh et al. [88] conducted a FEA of the adhesively bonded pipe joints by assuming both pipe walls and adhesive layer are linear elastic. Cognard et al.'s study [89] was concerned with increasing the performance of adhesively bonded cylindrical structures. Geometries which strongly limit the influence of edge effects were proposed. An optimization of the maximum transmitted load of cylindrical joints was also proposed using a pressure-dependent elastic limit of the adhesive.

The influence of stress-reduction methods on the strength of adhesively bonded joints composed of brittle adherends was studied by Vallée et al. [90]. Experimental and numerical investigations were carried out on two types of adherends: (a) fiber-reinforced polymers and (b) timber, considering three different stress-reduction methods: (i) adhesive roundings, (ii) chamfering and (iii) adhesive grading. The presented work allows for a better insight into the relation between stress reduction and strength increase of adhesively bonded joints, which are greatly affected by the brittleness of the adherends.

Nisar and Hashim's study [91] aimed to understand the failure of adhesive joints within glass fiber reinforced plastic pultrusions and the effects of molding materials on adhesion. This is based on experimental and numerical approaches with respect to molding and adhesive bonding and modeling of relatively small-scale laminates referred to as "meso". The analysis of the meso-scale models showed a good correlation with results from a macro-scale lap-shear model, in relation to transverse stresses in the composite.

Lavernhe et al. [92] proposed a behavioral model to describe tooth-adhesive-bracket devices, which can assess objectively and optimize the hardening of orthodontic bonds in different clinical situations. The results showed that the mechanical strength of the joint depends on the thickness of the adhesive, the specific position of the bracket on the vestibular side and the loading mode.

2.2. Stress singularity

Differences in mechanical properties between adherents and adhesive may cause stress singularity at the free edge of adhesively bonded joints. The stress singularity leads to the failure of the bonding part in joints. It is very important to analyze a stress singularity field for evaluating the strength of adhesively bonded joints. Fig. 5 shows the strength of singularities in lap joints. Although FEA is well suited to model almost any geometrical shape, traditional finite elements are incapable of correctly resolving the stress state at junctions of dissimilar materials because of the unbounded nature of the stresses. To avoid any adverse effects from the singularity point alternative approaches need to be sought.

A boundary element method and an eigenvalue analysis based on finite element method were used by Koguchi et al. [93–95] for evaluating the intensity of stress singularity. Stress singularity analysis for acting a delamination force to the specimen was carried out. Stress singularity field for the residual stresses varying material property in resin with temperature was determined. Combining the stress singularity fields for the delamination force and the residual thermal stress yielded a final stress distribution for evaluating the strength of interface. Kilic et al. [96] presented a finite element technique utilizing a global (special) element coupled with traditional elements. The global element includes the singular behavior at the junction of dissimilar materials with or without traction-free surfaces.

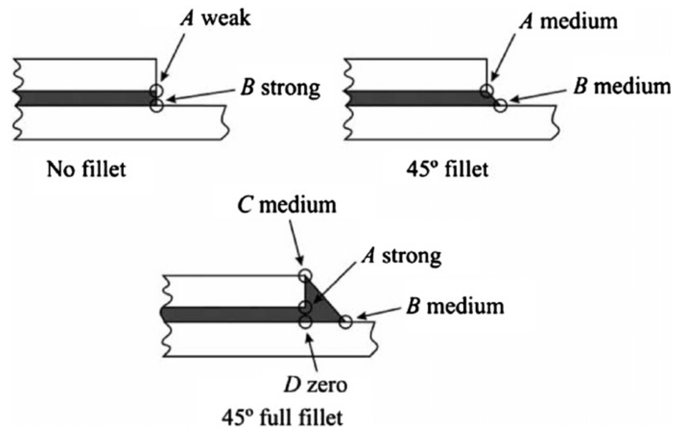

Fig. 5. Strength of singularities in lap joints [32].

In Kaneko and Narahashi's paper [97], adhesive strength criteria were investigated experimentally and analytically. Principal stress, principal strain and von Mises stress distributions at the adhesive interface of both the cylindrical butt joint specimens and the round bar butt joint specimens under the critical load were obtained by the elasto-plastic FEA using MARC. As a result, the mean value of von Mises stress distribution at the singularity area was found to be the most dominant factor of adhesive strength for the case with stress singularity area.

The adhesive strengths of glass fiber reinforced plastics/metal adhesive joints reinforced with glass mat under tensile shear loads and tensile loads were investigated by Iwasa [98] analytically and experimentally. The stress singularity parameters of the bonding edges were analyzed by FEA for various types of adhesive joints reinforced with glass mat. It was found that the shear stress and normal stress distributions near the bonding edge can be expressed by two stress singularity parameters.

To optimize the design of SLJs made by joining composite material to metals, the SLJs under both out-of-plane load and tensile load was examined by Shokrieh et al. [99]. By tapering the titanium adherend inside and outside, the stress distribution in the adhesive can be significantly changed at the tapered end and all three important stresses that governed the design (peel, axial and shear stress) were decreased for a joint under tension and out-of-plane load. A strain energy based on failure criteria was evaluated, which addressed the problem of stress singularities in FEA.

A stress singularity model was used by Van Tooren et al. [100] to predict joint failures in SLJs with varying bondline thickness. The critical stress intensity factor, or bondline toughness, was derived from the test data using an approximation formula for the change in external loading with bondline thickness. The resulting critical stress intensity factor combined with the calculated stress intensity factors gives a good prediction of the joint strength over a practical range of bondline thickness.

Goglio and Rossetto [101] explored recently the effects of the main geometrical features of an adhesive SLJ (subjected to tensile stress) on the singular stress field near to the interface end. Firstly an analysis on a bi-material block was carried out to evaluate the accuracy obtainable from FEA by comparison with the analytical solution for the singularity given by the Bogy determinant. Then the study on the SLJs was carried out by varying both macroscopic (bond length and thickness) and local (edge shape and angle) parameters for a total of 30 cases. It was confirmed that the angle play an important party in reducing the singular stresses.

The FEA, either under the assumption of linear elastic behavior or taking into account some aspects of the non-linear behavior of the adhesive, were carried out by Cognard [102] to study edge effects on a modified Arcan fixture. The results showed that the geometry of the substrate close to the edge of the joint and that the local geometry of the joint near the free edge are two important parameters in order to strongly limit the stress singularities for adhesively bonded joints.

Sawa et al. [103] carried out a two-dimensional stress analysis of adhesive butt joints with elastic circular fillers in the adhesive subjected to external tensile loadings. The effects of stiffness, location of filler particles and number of filler particles on the interface stress distributions and at the periphery of the filler particles were examined in the numerical calculations. It was observed that the difference in the interface stress distributions between the present analysis and 3-D FEA was substantial due to the stress singularity at the interfaces in the z-direction obtained from 3-D FEA.

2.3. Fracture

Identifying and interpreting the locus of failure, crack initiation and propagation behavior are significant aspects in evaluating the mechanical characteristics of adhesively bonded joints. While it is believed that materials always fail at the weakest location, the locus of failure, while closely related to material properties (such as tensile strength), quality of adhesion at the interface and fracture toughness of the bonds, depends also on the stress state at the crack tip [31].

In Hadavinia et al.'s research paper [104], FEA approach was used to model the crack advance through the adhesive layer in the elastic–plastic peel tests via a node-release technique, based upon attaining a critical plastic strain in the element immediately ahead of the crack tip. It was shown that this 'critical plastic strain fracture model (CPSFM)' results in predicted values of the steady-state peel loads which are in excellent agreement with the experimentally measured values. It is noted that the FEA CPSFM approach promises considerable potential for the analysis of peel tests which involve very extensive plastic deformation of the peeling arm and for analyzing, and predicting, the performance of more complex adhesively bonded geometries which involve extensive plastic deformation of the substrates. Fig. 6 shows the schematic of the meshes used for linear-elastic fracture-mechanics (LEFM) tapered double-cantilever beam (TDCB) specimen.

A closed form model predicting debond growth in composite flanged joints was proposed by Kim [105]. Such a model is useful for assessing the effects of partial debonds in adhesively bonded joints that are subjected to compressive loads. The model's accuracy was gauged by comparison of the strain energy release rate (SERR) profile prediction with the FEA based virtual crack closure technique (VCCT) calculations. Ueda et al. [106] investigated the effect of bond thickness on the fracture toughness and the strain field around a crack tip in adhesive joints using epoxy resin modified with solid rubber particles. The measured distributions of strains were compared with that estimated using the FEA in conjunction with Gurson's model. Ferraris et al.'s paper [107] presented the results of an experimental investigation on carbon/carbon composites (C/C) bonded joints tested in shear at room temperature, under seven different configurations. The FEA was performed to compare the stress distribution obtained within the joint for the different testing geometries. It was shown that the measured values of the apparent shear strength decrease with the maximum opening stress estimated within the middle of the joint.

The debonding of adhesive lap joints between FRP adherents was analyzed by Ascione and Mancusi [108] with regard to the influence of the chosen interface failure criterion. The numerical results of FEA were presented and discussed. Suggestions for the design of adhesive lap joints were also given. A 3D constitutive model was formulated by Iwamoto et al. [109] to describe the

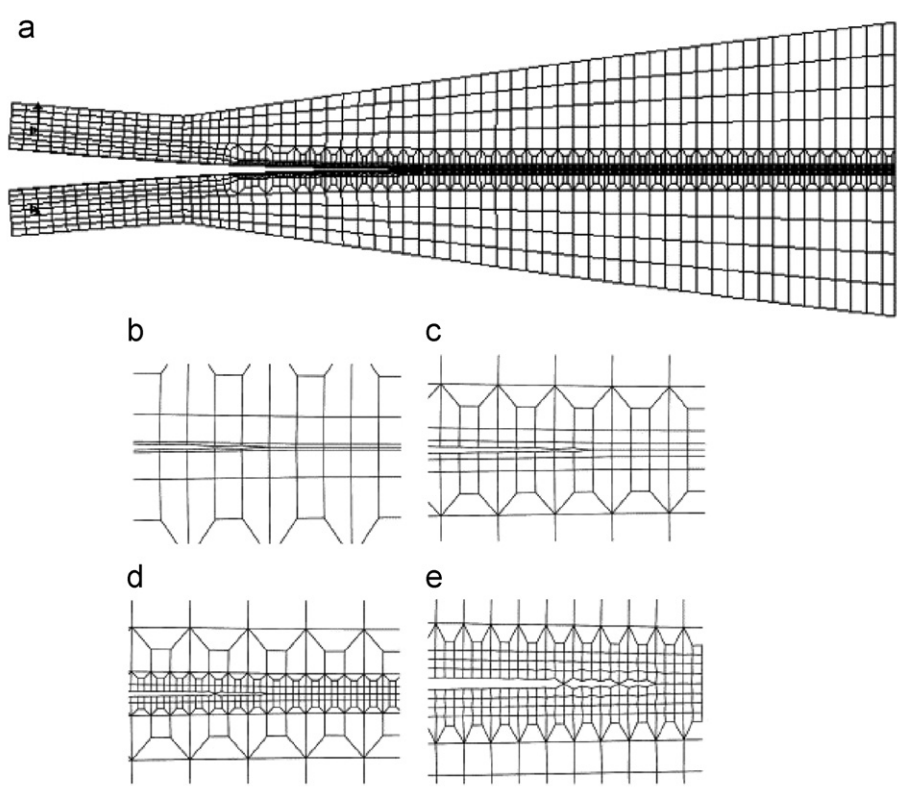

Fig. 6. Schematic of the meshes used for the LEFM TDCB specimen. (a) The overall representation and (b)–(e) represent the different elements sizes used for the meshes representing the adhesive layer: element sizes of 1.8, 0.6, 0.2, 0.1 mm, respectively [104].

deformation behavior of an epoxy resin structural adhesive in a wide range of strain rate. The formulated constitutive model was implemented into the commercial FE code ABAQUS/Explicit and then a computational simulation was performed. It was shown that the proposed model can be applied for a prediction of the deformation behavior of the different adhesives by comparing with experimental results.

By 3D FEA, Panigrahi and Pradhan [110] studied the behavior of embedded adhesion failure propagation in adhesively bonded single-lap laminated FRP composite joints clamped at one end and subjected to uniform extension at the other end. It was found that mode-II SERR is predominant in the propagation of such adhesion failures. The SERR values computed with respect to the adhesion failure lengths being propagated from the two ends of the adhesive layer are seen to be different. The 3-D non-linear FEA due to an in-plane loading was used by Panigrahi [111] to determine the out-of-plane normal and shear stresses over the critical surfaces of the adhesively bonded SLJs with FRP composite adherends.

Kahraman et al. [112] studied the influence of adhesive thickness and aluminum filler content on the mechanical performance of aluminum joints bonded by aluminum powder filled epoxy and found that the joints fail in cohesive mode due to the high stress levels generated in the adhesive, which indicates that the adhesion to the metal surface is stronger than that of the interior part of the adhesive.

Wang and Zhang [113] presented new analytical solutions for the energy release rate and for the phase angle of the interface crack in sandwich structures or adhesively bonded joints. Comparisons with existing solutions and FEA suggested that the new models provide enhanced accuracy due to consideration of the effect of shear deformation.

In Lu et al.'s paper [114], a new anisotropic yield criterion which is determined from tensile and shear tests, was developed and incorporated into the FEA to predict the static load–displacement curves of various adhesive bonded steel joints. The results shown that for the joints made of dissimilar steel grade and sheet gage, the stiffness (i.e. strength and thickness) of the two adherends should be balanced for obtaining the optimum joint strength.

Esmaeel and Taheri [115] investigated the effect of delamination on the structural response of an adhesively bonded tubular joint with composite and aluminum adherends. The FEA was used to conduct a parametric investigation. Results provided interesting insight into the effect of an interlayer delamination on the stress distribution within the adhesive.

Choupani [116] carried out FEA on modified Arcan specimens with different adherends for determining the fracture toughness KIC and KIIC for a range of substrates under mixed-mode loading conditions. Another goal was to study the relationship between the stress intensity factors and the fracture toughness.

Shahin and Taheri [117] proposed an analytical model to determine the SERR in adhesive joints of various configurations such as the double-cantilever beam and SLJs. Closed-form solutions were presented for balanced and unbalanced joints under mode I, II and mixed-mode I/II that take into account the influence of the shear force both on the adhesive stresses and the SERR. Results from the proposed analytical model were in good agreement with FEA results and with analytical models found in the literature.

Campilho et al. [118–122] studied systematically the failure behavior of repaired composite laminates under different geometric changes. The ABAQUS numerical models and a developed cohesive mixed-mode damage model were used to carry out the failure analysis.

In Das and Pradhan's paper [123], FEA results of the bonded tubular single-lap joint (TSLJ) were compared with those available in literature and were found to be in good agreement. Failure indices at different critical interfaces were evaluated using quadratic failure criterion within the adhesive and Tsai-Wu coupled stress criterion for the adherend adhesive interfaces. Based on the later criteria, locations prone to adhesion failure initiation were identified to be existing at the interface of the loaded tube and the adhesive at the edge of the overlap length nearer to the clamped end of the TSLJ.

An one-parameter viscous regularization of the softening adhesive material law was used by Schmidt and Edlund [124] for improving the numerical behavior. The discrete adhesive material law was formulated and the matrix expressions needed for implementation of an eight-node FE were derived. A number of numerical examples were presented where the progressive growth of damage and failure loads were studied and where the numerical improvements from using a rate-dependent adhesive material model were exemplified.

2.4. Damage modeling

Damage modeling approach is being increasingly used to simulate fracture and debonding processes in adhesively bonded joints. The techniques for damage modeling can be divided into either local or continuum approaches. In the continuum approach the damage is modeled over a finite region. The local approach, where the damage is confined to zero volume lines and surfaces in 2-D and 3-D, respectively, is often referred to as cohesive zone approach [32].

In Ouyang and Li's studies [125,126], Cohesive Zone Model (CZM) based analytical solutions were obtained for the bonded pipe joints under torsion. An integral form based general expression was derived which is suitable for arbitrary type of non-linear cohesive laws. It was found that, when the bond length of the pipe joint is large enough, the torsion load capacity is indeed independent of the shape of cohesive laws and the bond length. Good agreement with FEA result validates the accuracy of the current model.

In subsequent study, a natural boundary condition based method was proposed by Ouyang and Li [127], and thus the concept of extended crack length is no longer required and more realistic and natural local deformation beyond crack tip can be obtained. The non-linear response in both the ascending and descending stages of loading is accurately predicted by the current method, as evidenced by a comparison with both experimental results and FEA results. This method can be extended to multilinear cohesive laws as well.

A new data reduction scheme was proposed by de Moura et al. [128,129] for measuring the critical fracture energy of adhesive joints. The method is based on the crack equivalent concept and does not require crack length monitoring during propagation, which is very difficult to perform accurately in these tests. The method accounts for the fracture process zone effects which can be significant when ductile adhesives are used.

Sun et al.'s work [130] showed that a CZM has to be modified to include coupling between normal and shear modes of deformation when there is extensive shear deformation of the adhesive layer. A suitable CZM strategy was described, and the mode-II cohesive parameters determined from the model were presented as a function of loading rate. Based on CZM and FEA, the relationship between fracture load and adhesive properties was investigated by Lee et al. [131] in adhesively bonded joint tensile test and T-peel test.

A new approach was developed by Fan et al. [132] to implement the cohesive zone concept for the simulation of delamination in fiber composites or crack growth in adhesive joints in tension or shear mode of fracture. Multi-axial-stress criterion was used to govern the damage initiation so that the model is able to show the hydrostatic stress effect on the damage development. The damage material model was implemented in a finite element model consisting of continuum solid elements to mimic the damage development.

Martiny et al. [133] carried out numerical simulations of the steady-state fracture of adhesively bonded joints in various peel test configurations. The model was based on a multiscale approach involving the simulation of the continuum elasto-plastic response of the adherends and the adhesive layer, as well as of the fracture process taking place inside the adhesive layer using a cohesive zone formulation.

Based on CZM concepts, Alfano et al. [134] studied the mode I fracture in adhesively bonded joints. An intrinsic piece-wise linear cohesive surface relation was used for modeling fracture in a pre-cracked bonded double-cantilever beam (DCB) specimen, Finite element implementation of the CZM was accomplished by means of the user element (UEL) feature available in the ABAQUS code. The sensitivity of the cohesive zone parameters (i.e. fracture strength and critical energy release rate) in predicting the overall mechanical response was examined.

3. Environmental behavior of adhesively bonded joints

Structural adhesives are generally thermosets such as acrylic, epoxy, polyurethane and phenolic adhesives. They will be affected by environmental conditions and exhibit time dependent characteristics. The lifetime of adhesive joints are difficult to model accurately and their long-term performance cannot easily and reliably be predicted, especially under the combined effects of an aggressive environment and mechanical loading.

3.1. Moisture effects on adhesively bonded joints

In the experiments, it is found that the strength of adhesive joints decreased as a function of the time for which the samples are in a humid environment. The adhesives absorb moisture more than most substrate materials and expand more because of the moisture. Water may affect both the chemical and physical characteristics of adhesives and also the nature of the interfaces between adhesive and adherends.

A mixed mode interfacial rupture element with the separation law was proposed by Crocombe et al. [135] to simulate interfacial fracture failure of the joints exposed to various ageing environments. The two moisture-dependent fracture parameters, fracture energy and tripping traction, were calibrated using a mixed-mode flexure (MMF) test and FEA. The plasticity of the substrates was incorporated successfully and the predicted joint residual strengths agree well with the corresponding experimental data. Using the elasto-plastic FEA, Li et al. [136] studied the influence of the water absorption on the stress distribution in the polyacrylate adhesive layer of the SLJs. The results from the numerical simulation showed that the peak stress at the corner of the fillet decreased evidently as the moisture absorption level increased.

A finite element-based methodology incorporating moisture history was developed by Mubashar et al. [137] to predict the cyclic moisture concentration. A comparison was made between the new modeling methodology and a similar method that neglects the moisture history dependence. It was found that the concentration predictions based on non-history dependent diffusion characteristics resulted in over-prediction of the moisture concentration in cyclic conditioning of adhesive joints.

The use of CZM to predict the long-term durability of adhesively bonded structures exposed to humid environments was investigated by Liljedahl et al. [138]. The joints were exposed to high relative humidity (RH) environments and immersion in both tap and deionised water for up to a year before quasi-static testing to failure. In the model, the cohesive zone parameters determine the residual strength of the joints. The degradation of these parameters was related directly to the moisture concentration. The model was then extended to include degradation due to stress and more corrosive environments.

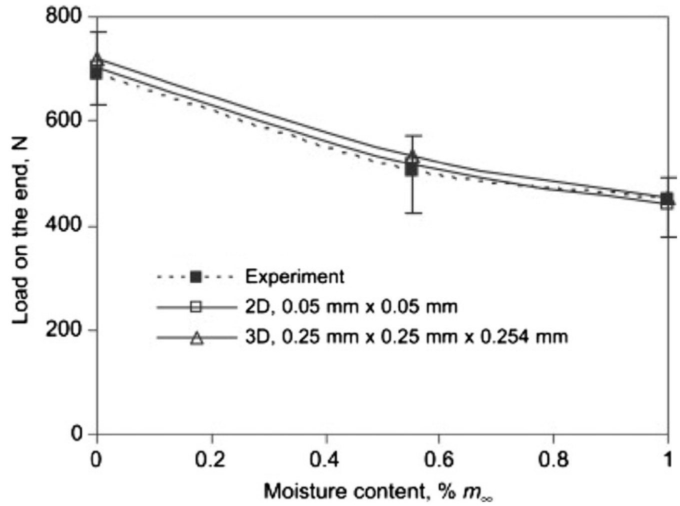

Fig. 7. Predicted failure loads from the 2-D and 3-D MMF models using the continuum damage model with the different mesh sizes [141].

Tsai et al. [139] investigated the effect of moisture ingression on stress field of the chip-on-glass (COG) packages with the non-conductive film (NCF) adhesively bonding. The coefficients of moisture diffusion and the hygro-strains of the NCF adhesive were determined by an innovative approach of measuring the out-of-plane deformation of the bi-material specimens during moisture absorption at the condition of 30 °C/85%RH using Twyman–Green interferometry, associated with FEA and bi-material theory. After being validated by the diffusion theory, the moisture-transient FEA reveals that the moisture absorption of the COG package under 30 °C/85%RH is nearly saturated after 1000 h. It was also found that there are large tensile stresses at pad corner and mediate ones across bump joint, and these tensile stresses gradually increase with moisture absorption and up to the maximum at the state of moisture saturation.

A progressive cohesive failure model was proposed by Hua et al. [140,141] to predict the residual strength of adhesively bonded joints using a moisture-dependent critical equivalent plastic strain for the adhesive. A single, moisture-dependent failure parameter, the critical strain, was calibrated using an aged, mixed-mode flexure (MMF) test. The FEA package ABAQUS was used to implement the coupled mechanical-diffusion analyses required. Fig. 7 shows the predicted failure loads from the 2D and 3D MMF models using the continuum damage model with the different mesh sizes. This approach has been extended to butt joints bonded with epoxy adhesive. This involves not only a different adhesive and joint configuration but the high hydrostatic stress requires a more realistic yielding model [142].

3.2. Temperature effects on adhesive joints

In Aydin et al.'s study [143], the tensile load capabilities of the SLJs bonded with a flexible adhesive that possesses pressure-sensitive properties were experimentally investigated with respect to the applied pressure during the curing operation, and the experimental results were compared with the FEA results. A detailed series of experiments and FEA were carried out by Grant et al. [144] to assess the effects of temperature that an

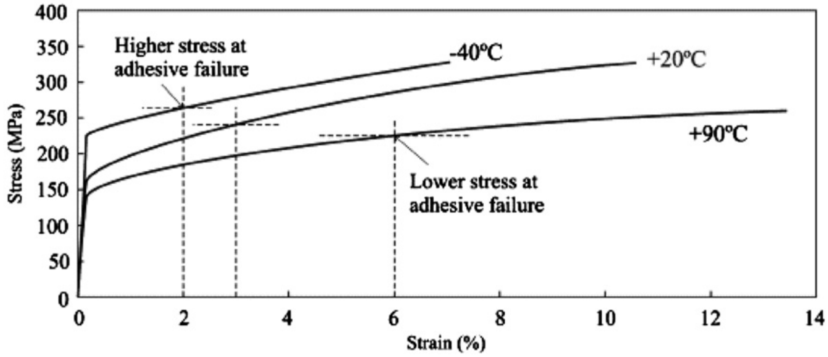

Fig. 8. Stress–strain curves for sheet steel at −40, +20 and +90 °C along with the adhesive strain to failure at the corresponding temperatures [144].

automotive joint might experience in service. Tests were carried out at −40 and +90 °C. It was shown that the failure criterion proposed at room temperature is still valid at low and high temperatures, the failure envelope moving up and down as the temperature increases or decreases, respectively. Fig. 8 shows the stress–strain curves for sheet steel at −40, +20 and +90 °C along with the adhesive strain to failure at the corresponding temperatures.

In Zhang et al.'s recent work [145], quasi-static tensile behavior of adhesively bonded double-lap joints, composed of pultruded GFRP laminates and an epoxy adhesive, was investigated under temperatures ranging between −35 and 60 °C. They found that the failure mechanism changed with increasing temperature from fiber-tear to adhesive failure. The modeling results obtained using existing empirical models and FEA compared well to the experimental data in the examined temperature range. Apalak and Gunes [146] investigated 3D thermal residual stresses occurring in an adhesively bonded functionally graded SLJ subjected to a uniform cooling. They concluded that the free edges of adhesive–adherend interfaces and the corresponding adherend regions are the most critical regions, and the adherend edge conditions play more important role in the critical adherend and adhesive stresses.

da Silva et al. [147–151] investigated systematically the mechanical properties of the mixed-adhesive joints, which are joints with a combination of a low-temperature adhesive and a high-temperature adhesive. Using an integrated combination of mechanical property evaluation and FEA, Speth et al. [6] described a logical method for the design and certification of adhesively bonded composite to steel joints for the marine industry. Calculated factors of safety for the sandwich design used here show that the joint has adequate strength to maintain structural integrity even after severe environmental exposure.

Malvade et al.'s work [152] focused on simulation of non-linear mechanical behaviors of adhesively bonded double-lap shear (DLS) joints for variable extension rates and temperatures. It was shown that the shell-solid model can effectively predict the mechanical behavior of the joint. Exponent Drucker–Prager or von Mises yield criterion together with non-linear isotropic hardening was used for the simulation of DLS joint tests.

4. Fatigue loading analysis

Fatigue loading is a common cause of failure in adhesively bonded joints. For adhesives, the presence of this type of loading is found to lead to a much lower resistance to crack growth than under monotonic loading. The fatigue behavior of adhesively bonded joints needs a significant research improvement in order to understand the failure mechanisms and the influence of parameters such as surface pre-treatment, adhesive thickness or adherends thickness.

4.1. Stress analysis

In a recent study, Jen and Ko [153] investigated the effect of bonding dimensions on fatigue strength. The FEA was adopted to obtain the local stress states at the interface between the adhesive and the adherend. Three selected parameters, namely maximum interfacial peeling stress, maximum interfacial shear stress and a linear combination of interfacial peeling stress and shear stress, were considered to correlate with the fatigue life data of all specimens with various adhesive dimensions.

Results of fatigue tests on adhesive lap joints of thick (9.9 mm) composite laminates were presented and discussed by Bernasconi et al. [154]. Specimens of different overlap length, different shape, and different materials were tested. In order to investigate the relationship between peak elastic stresses in the adhesive layer and fatigue life, a 2-D structural FEA was performed.

A research study on the fatigue behavior of aluminum alloy adhesive lap joints was carried out by Pereira et al. [155] to understand the effect of surface pre-treatment and adherends thickness on the fatigue strength of adhesive joints. The fastest fatigue damage was related with a high surface roughness and a high stress perpendicular to adhesive surface. The FEA was also performed to understand the effect of the adherends thickness on the stress level. Square elements were used to optimize the accuracy of the FEA.

In Quaresimin and Ricotta's paper [156], linear elastic FEA were carried out to evaluate generalized stress intensity factors (SIFs) in the geometry of interest and the influence of overlap length, corner geometry, adhesive properties and thickness was investigated. Geometric non-linear analyses were instead used for the analysis of the SERR trends as a function of the crack length. On the basis of these results, a new equivalent formulation for the SERR was introduced, suitable to account for the mixed-mode loading condition as well as for the continuous variation of the mode-mixity during the fatigue life of the joints.

A method of repair was proposed by Bachir Bouiadjra et al. [157]. It consisted in dividing the adhesive layer into two bands with different properties. The first band was used on the crack region to ensure the stress transfer and the second band was used beyond the crack region to avoid the adhesive failure. The results showed that the energy release rate at the crack tips is highly reduced by the difference of properties between the two adhesive bands, what can involve the improvement of fatigue life of cracked structure.

FEAs were conducted by Wang et al. [158] for double lap, metal-to-metal bonded repair joints with different linear edge taper angles, or optimal taper profiles using the shape optimization approach.

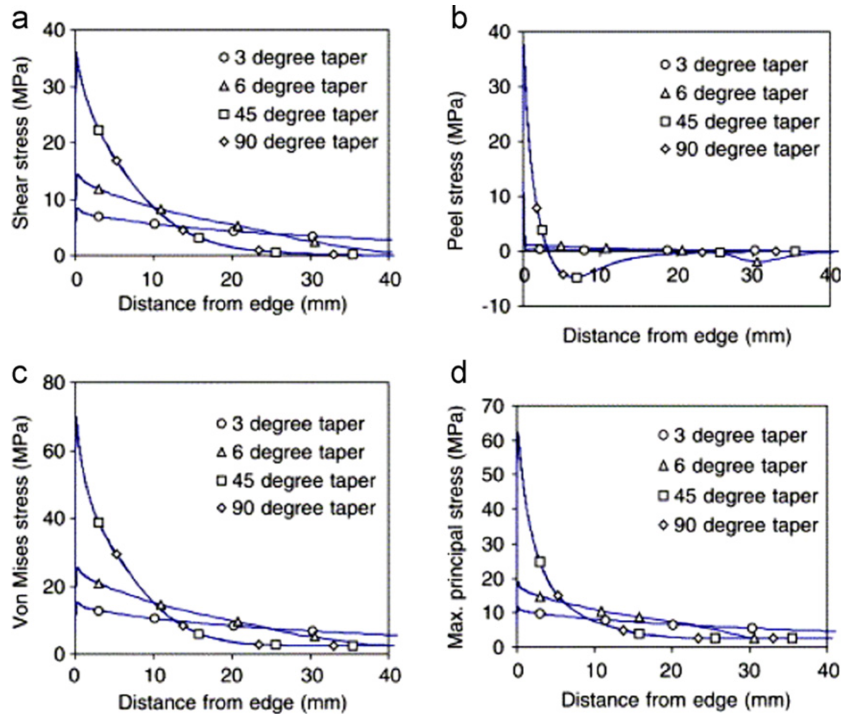

Fig. 9. Stresses distribution along middle layer of adhesive layer under different taper angles (19.2 kN load) [158].

The results predicted that the taper angle should strongly affect the fatigue performance of the repair patch. Compared with the 90° taper case, the peak stresses in the 6° taper case reduced by around 60%, and the stresses in the 3° taper case reduced by around 80%. The optimum design was able to reduce the peak stresses by about 50% compared with the widely used 6° linear taper (i.e. 1:10) with the same taper length. Thus, it appeared to be the best in terms of the fatigue resistance vs. taper region length. Fig. 9 shows the stresses distribution along middle layer of adhesive layer under different taper angles.

The tests were carried out by Ferreira et al. [159] on specimen joints manufactured using different stacking sequences: solely bi-directional woven E-glass fibers and polypropylene composites; and hybrid stacked composites. The main objective of the work was to improve the fatigue strength using hybrid fiber composites with a polypropylene/hemp natural fiber layer adjacent to the bond interface which was expected to produce more uniform stresses in transient regions.

The fatigue behavior of adhesive joints made with commercially coil-coated thin aluminum sheets was measured by Datla et al. [160] using modified DCB and cracked lap shear (CLS) specimens that avoided yielding. Experimental and the FEA demonstrated that the reinforcing adhesive layer had an insignificant effect on the stress state at the crack tip and the resulting fatigue behavior. It was observed that the phase angle affected the threshold SERR and the crack growth rates.

4.2. Fatigue damage modeling

An elasto-plastic damage model was proposed by Graner Solana et al. [161] for predicting the experimentally observed backface strain patterns and fatigue life at different fatigue loads. The FEA code ABAQUS and a user defined subroutine were used to calculate the damage, the resultant degradation in adhesive Young's modulus and yield stress. A procedure to predict fatigue crack growth in bonded joints was developed recently by Pirondi and Moroni [162] within the framework of CZM and FEA. The idea is to link the fatigue damage rate in the cohesive elements to the macroscopic crack growth rate through a damage homogenization criterion.

Fessel et al.'s paper [163] assessed the fatigue performance of reverse-bent joints. Results from analysis demonstrated that significant improvements could be achieved. The paper also explained the failure mechanism of the joints under fatigue loading. The propagation of an interface crack subjected to mixed-mode I/II was investigated by Marannano et al. [164] for Al–Al bonded joints. The analytical SERR was compared by the FEA using the virtual crack closure technique (VCCT). Several fatigue crack growth tests were carried out in a plane bending machine to compare the experimental energy release rates to those of the analytical and FEA solutions. Fatigue crack propagation behavior of adhesively bonded CFRP/aluminum joints was investigated by Ishii et al. [165]. A FEA was conducted to investigate the mode ratio, and stress and strain distributions near the crack tip. The effect of the adherend thickness on the crack propagation rate was tentatively explained in terms of stress distributions near the crack tip and crack propagation path.

The backface strain (BFS) measurement technique was used by Shenoy et al. [166] to characterize fatigue damage in the SLJs subjected to constant amplitude fatigue loading. Different regions in the BFS plots were correlated with damage in the joints through microscopic characterization of damage and cracking in partially fatigued joints and comparison with 3D FEA of various crack growth scenarios. In Shenoy et al.'s recent study [167], a unified fatigue methodology (UFM) was proposed to predict the fatigue behavior of adhesively bonded joints. In this methodology a damage evolution law is used to predict the main parameters governing fatigue life. The model is able to predict the damage evolution, crack initiation and propagation lives, strength and stiffness degradation and the BFS during fatigue loading. The model is able to unify previous approaches based on total life, strength or stiffness wearout, BFS monitoring and crack initiation and propagation modeling. Fig. 10 shows the extended L–N curve using UFM and fracture mechanics. It can be seen that the UFM

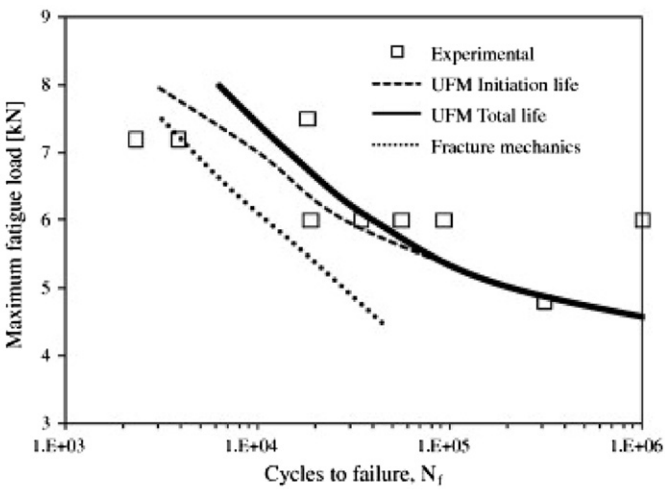

Fig. 10. Extended *L–N* curves using UFM and fracture mechanics [167].

approach, which accounts for both initiation and propagation can provide a good prediction of the total fatigue life at all loads.

In Wahab et al.'s study [168], the damage parameters for crack initiation in a SLJ were determined by combining continuous damage mechanics, FEA and experimental fatigue data. They found that the effect of stress singularity, due to the presence of corners at edges, also contributes to the complex state of stress and to the variability of the triaxiality function along the adhesive layer in a SLJ. Keller and Schollmayer [169] studied the through-thickness performance of adhesive joints between pultruded FRP bridge decks and steel girders experimentally and numerically. They concluded that the joint ultimate loads could be accurately predicted based on stress concentration factors from FEA and FRP through-thickness tensile strength values obtained from small-scale coupon tests. They also found that the fatigue loading up to 10 million cycles showed no stiffness degradation.

The FEA were performed by Hosseini-Toudeshky et al. [170] to investigate the crack propagation of single-side repaired panels using composite patches containing an initial central inclined crack. In these analyses the general mixed-mode fracture conditions of modes I, II and III and the real three-dimensional crack-front were considered in the finite element crack growth modeling. For this purpose, modified virtual crack closure technique (MVCCT) was used to calculate the three SERR components corresponding to various fracture modes at the crack-front.

The effect of load ratio on the fatigue behavior of adhesively bonded joints was investigated by Khoramishad et al. [171] using both experimental and numerical approaches. A numerical model that accounts for the load ratio effect in constant amplitude fatigue loading was developed to predict the response of SLJs. Damage initiation and propagation phases were monitored using the back-face-strain and in-situ video-microscopy techniques. The load ratio effect on the fatigue behavior of adhesively bonded joints was successfully predicted using a strain-based fatigue damage model.

5. Dynamic loading analysis

In the design of mechanical systems, which incorporate jointed components, for minimum vibration response, a specific knowledge of the dynamic behavior of the component materials and joints is important. Adhesive bonding offers advantages on acoustic isolation and vibration attenuation relatively to other conventional joining processes. It is believed that adhesively bonded joints act to augment the system damping capacity.

5.1. Structural damping

Mechanical structures assembled by adhesively bonding are expected to possess a high damping capacity because of the high damping capacity of the adhesives. Investigations have been carried out for clarifying the damping characteristics of adhesively bonded structures and to establish an estimation method for the damping capacity.

Ghoneam et al. [172] carried out dynamic analysis of adhesively bonded joint for composite structures to investigate mainly the influences of bonded adhesive line configuration and boundary condition on the dynamic behavior of the test specimens. It was found that the damping capacity is proportional to the stiffness of the bonded joint specimens. The type of the proportionality depends mainly on the bond line configuration type, lamina orientation, and boundary conditions. This in turn enables an accurate evaluation for selecting the proper characteristics of the specimens for controlling the present damping capacity and the proper resistance against deformation during the operating process.

In a research paper by Apalak and Yildirim [173], the 3D transient vibration attenuation of an adhesively bonded cantilevered SLJ was controlled using actuators. The transient variation of the control force was expressed by a periodic function so that the damped vibration of the SLJ was decreased. Optimal transient control force history and optimal actuator position were determined using the Open Loop Control Approach and Genetic Algorithm. In a similar work by Apalak et al. [174], the response of an adhesively bonded double containment cantilever joint subjected to a transverse excitation force was measured with a contactless eddy-current sensor and the first bending natural frequency was determined using the Fast Fourier Transform method. The damped free vibration analysis was carried out using the FEA and its measured loss factor.

Pandurangan and Buckner [175] proposed an experimental technique to diagnose damage in single-lap adhesive joints subject to cyclical tensile loading. Vibration analysis revealed that damage can be correlated with changes in identified modal damping ratios. Constant amplitude forcing functions were employed to eliminate amplitude-dependent non-linearities in the dynamic response profiles. Damping estimates obtained from time-domain analyses correlate well with damage magnitudes.

Recent work by He [176] studied the influence of adhesive layer thickness on the dynamic behavior of the single-lap adhesive joints. The results showed that the composite damping of the single-lap adhesive joint increases as the thickness of the adhesive layer increases.

Effects of various dynamic characteristics in the adhesively bonded joints subjected to dynamic forces were investigated by Kaya et al. [177] using 3D FEA. The joint was modeled as a thin plate clamped from the left side. The in-plane vibration analysis was constructed. First, the natural frequencies and mode shapes are obtained, and then point and transfer receptances were extracted, employing structural damping. It was observed that the damping greatly decreased the resonance amplitudes.

Bartoli et al. [178] proposed a semi-analytical finite element (SAFE) method for modeling wave propagation in waveguides of arbitrary cross-section. The general SAFE technique was extended to account for viscoelastic material damping by allowing for complex stiffness matrices for the material. The dispersive solutions were obtained in terms of phase velocity, group velocity (for undamped media), energy velocity (for damped media), attenuation and cross-sectional mode shapes. The proposed SAFE formulation was applied to several examples, including anisotropic viscoelastic layered plates, composite-to-composite adhesive joints and railroad tracks.

In Kim et al.'s study [179], L-shaped joint for combining bed and column of the micro-EDM (electrical discharge machining) machine was proposed and fabricated using adhesive bonding. The dynamic performance such as damping characteristics was investigated by vibration tests and FEA. From the results optimal configuration and materials for high precision micro-EDM machines were proposed.

5.2. Modes of vibration

With the increase in the use of adhesively bonded joints in primary structures, such as aircraft and automotive structures, reliable and cost-effective techniques for structural health monitoring (SHM) of adhesive bonding are needed. Modal and vibration-based analysis, when combined with validated FEA, can provide a key tool for SHM of adhesive bonding.

In an early paper, He and Oyadiji [180] investigated in detail the influence of the characteristics of structural adhesives on the transverse free vibration of single-lap cantilevered beam joints and found that the transverse natural frequencies of the joints increase with increasing adhesive Young's modulus whereas any significant change was not observed with increasing Poisson's ratio.

Using 3D FEA and the back-propagation ANN method, Apalak et al. [181] studied the 3D free vibration behavior of an adhesively bonded corner joint with single support. They found that the support length, plate thickness and joint length all played important roles in the natural frequencies, mode shapes and modal strain energies of the corner joint. The Genetic Algorithm was also combined with the present ANN models in order to determine the optimum geometrical dimensions which satisfied the maximum natural frequency and minimum modal strain energy conditions for each natural frequency and mode shape of the adhesively bonded corner joint. By the same methods, Apalak and Yildirim [182] investigated the effects of fiber angle, fiber volume fraction, overlap length, and plate thickness on the natural frequencies and the mode shapes of the adhesive joint. The ANN models indicated that the fiber angle is a more dominant parameter than the fiber volume fraction on the natural frequencies and the corresponding mode shapes of the adhesive joint, and the plate thickness and the overlap length are important geometrical design parameters whereas the adhesive thickness has a minor effect.

In He's work [183], the ABAQUS FEA software was used to predict the natural frequencies, mode shapes and frequency response functions (FRFs) of adhesively lap-jointed beams. In the case of forced vibration of the single lap-jointed cantilevered beam, the dynamical response of the free edge is most important because it fully represents the dynamical characteristic of the beam. Nodes 151, 153 and 155 in Fig. 11 are the nodes at the two corners and center of the free edge of the beam (the corresponding nodes in the FE mesh are 60621, 2060621 and 4060621, respectively). It was found that the measured FRFs are close to the predicted FRFs for the first two modes of vibration of the beam. Above the second mode of vibration, there is considerable discrepancy between the measured and predicted FRFs. Fig. 12 shows the FRFs predicted by FEA and measured using the test rig.

Apalak and Yildirim [184] reported the most effective design parameters for the 3D free vibration and modal stress state of an adhesively bonded cantilevered composite tubular single-lap joint. The effects of fiber angle, fibre volume fraction, overlap length, tube

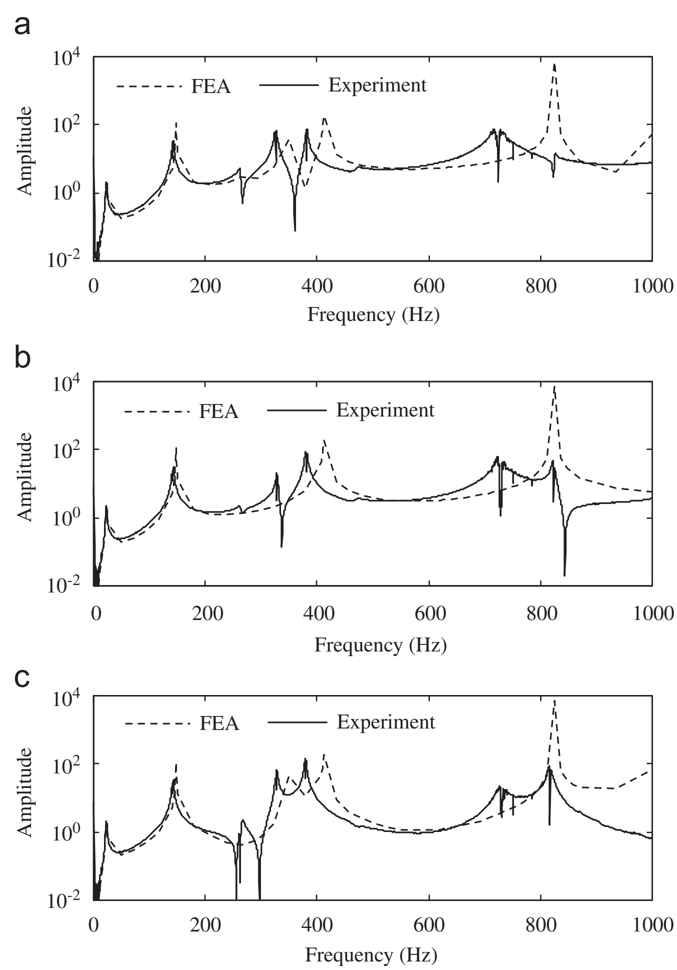

Fig. 12. FRFs predicted by FEA and measured using the test rig [183](a) FRF for node 60621 &151, (b) FRF for node 2060621 &153 and (c) FRF for node 4060621 &155.

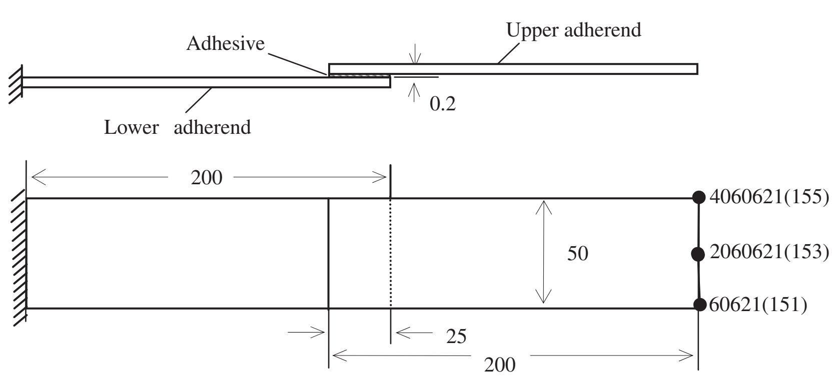

Fig. 11. Location of nodes at the free edge of the single lap-jointed cantilevered beam [183].

thicknesses and inner tube radius on the first ten natural frequencies and mode shapes of the adhesive tubular joint were investigated, using the back-propagation ANN method. The FEA was used for random values of the design parameters. The ANN models indicated that increasing each of all the design variables resulted in increases in the first ten natural frequencies as well as in the modal strain energies, whereas increasing the inner tube thickness reduced the natural frequencies but increased the modal strain energies.

Three-dimensional free vibration and stress analyses of adhesively bonded functionally graded SLJs were carried out by Gunes et al. [185]. The effects of the adhesive material properties, such as modulus of elasticity, Poisson's ratio and density were found to be negligible on the first ten natural frequencies and mode shapes of the adhesive joint. Both the FEA and the back-propagation ANN method were used to investigate the effects of the geometrical parameters, such as overlap length, plate thickness and adhesive thickness; and the material composition variation through the plate thickness on the natural frequencies, mode shapes and modal strain energy of the adhesive joint.

In a recent study, Gunes et al. [186] investigated the free vibration behavior of an adhesively bonded functionally graded SLJ, which composed of ceramic (Al_2O_3) and metal (Ni) phases varying through the plate thickness. The effects of the similar and dissimilar material composition variations through-the-thicknesses of both upper and lower plates on the natural frequencies and corresponding mode shapes of the adhesive joint were investigated using both the FEA and the back-propagation ANN method. A series of the free vibration analyses were carried out for various random values of the geometrical parameters and the through-the-thickness material composition so that a suitable ANN model could be trained successfully.

5.3. Impacting

Impact fracture of an adhesive layer in a structure was analyzed by Carlberger and Stigh [187]. Three constitutive models of the adhesive layer were used in analysis. It was shown that an amplification of the strain rate is achieved in the adhesive layer. It was also shown that an artificially increased flexibility of the adhesive in an aluminum structure gives only minor influences of the general behavior.

In Sawa et al.'s paper [188], the strength of adhesively bonded joints subjected to impact shear loading was investigated using modified split Hopkinson pressure bar (SHPB) apparatus. The stress distributions in the joints subjected to impact shear loading were simulated by the FEA. A stress distribution of the adhesive layer in the pin-color specimen under an impact shear load was numerically studied by Iwamoto et al. [189]. A finite element simulation with 3D constitutive model was performed under an impact loading condition. The joint strength was experimentally evaluated in a wide range of deformation rate by using an INSTRON-type material testing machine and a SHPB apparatus.

Park and Kim [190] investigated the high velocity transverse impact of composite joints by hailstones. The damage areas imaged by ultrasonic scanning were quantitatively measured and the specimens were also sectioned and observed with optical microscopy to determine the exact location of damage. The FEA of the impact was conducted and the results showed that the plies where delaminations were observed to occur have the highest peel and shear stresses.

Silberschmidt et al. [191] studied the effect of repetitive low-energy impacting (known as impact fatigue) on reliability and crack growth in adhesively bonded joints. The impact fatigue was compared to the standard tensile fatigue in order to assess severity of such loading regime. Crack propagation in a joint exposed to these types of loading was studied experimentally and by FEA.

Using 3D FEA, Challita and Othman [192] simulated the SHPB tests on double-lap bonded joints. The study focused on the influence of material, geometrical and dynamic parameters on the SHPB accuracy and concluded that the SHPB bar method gives a good estimation of the mean adhesive stress value. However, its estimation, to the mean adhesive strain and to the maximum adhesive stress and strain, was rather bad. A unified parameter was therefore proposed to help designing specimens and to correct the SHPB results.

The stress variations and stress distributions in stepped-lap adhesive joints of dissimilar adherends under impact tensile loadings were analyzed by Sawa and Ichikawa [193] in elastic range using 3D FEA. The impact loadings were applied to the lower adherend by dropping a weight. As the results, the maximum value of longitudinal stress increased as Young's modulus of the adherends increased for the impact loadings. In addition, the experiments to measure the strain response of joints subjected to impact tensile loadings were carried out using strain gauges.

The response of a balanced SLJ to a transverse normal impact load was investigated by Vaidya et al. [194] using LS-DYNA 3D FEA and supporting experiments. The stress distribution in the adhesive layer for a transverse impact load was observed to be asymmetric. It was found that the cohesive failure of the joint always initiated from the adhesive edge under tensile stress. Experiments involving low velocity impact (LVI) tests were carried out on the bonded joint to verify the results from the finite element model. Fig. 13 shows the schematic of setup for the low velocity impact testing of the joint and Fig. 14 shows the meshing scheme.

Kim et al. [195] carried out transverse impact tests on adhesively bonded glass-epoxy lap joints to determine the modes of damage resulting from out-of-plane impacts to the overlap region and to identify mechanisms by which damage formation

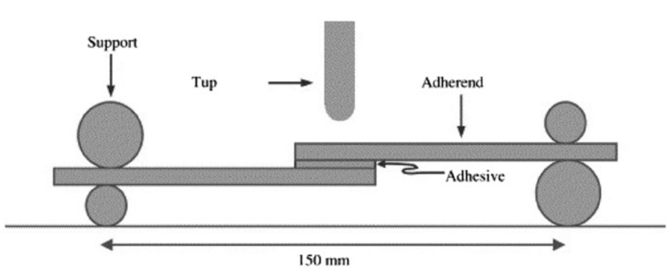

Fig. 13. Schematic of setup for the low velocity impact testing of the joint [194].

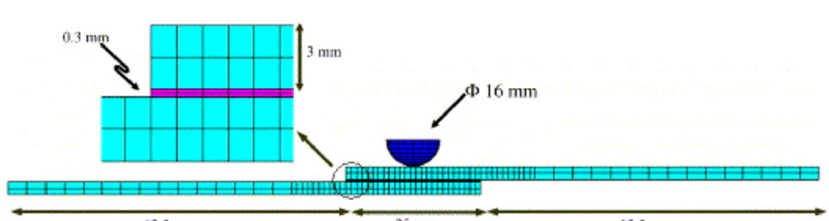

Fig. 14. Meshing scheme used for simulating the impact condition in LS-DYNA [194].

occurs. Impacts over an energy range 10–50 J were produced using a low-velocity and high-mass drop weight tower. Localized debonding was observed for lower energy impacts in the region surrounding the impact point. The FEA was used to determine the stresses that develop in the adhesive during impact, and to corroborate experimentally based conclusions on the mechanisms of damage formation.

6. Hybrid joints

It is also important for bonding process to benefit from the advantages of other joining techniques, such as spot welding, self-piercing riveting (SPR), clinching, etc. These can be done by combining bonding process with other joining techniques and are referred to as hybrid joining processes. A number of researchers have carried out mechanical performances of the hybrid joints in different materials with various load conditions. Their study shows that the combination produced a much stronger joint in both static and fatigue tests.

6.1. Weld-bonded hybrid joint

Three-dimensional viscoplastic FEA of a single-lap weld-bonded joint were conducted by Yin et al. [196] to investigate the stress redistribution. The results showed that the stress concentration factor of weld-bonded joint is significantly lower than that of the direct spot-weld in connection. The simulations also illustrated that increasing of creep parameter will enhance the maximum stress level in the weld spot. Based on the linear elasticity theory considering the adherend shear deformations, the stress and stiffness models of a weld-bonded SLJ were developed by Zhao and Yue [197]. The shear stress along the overlap and longitudinal normal stress of the upper adherend in the analytical solutions were obtained and compared with the numerical solutions determined by the 2-D FEA. Darwish et al. [198–201] studied systematically the most influential parameters governing the strength of weld-bonded joints. Fig. 15 shows the finite-element model for weld-bonded joint. The thermal stresses developed in joints, the thickness and elastic modulus of adhesive, the stress concentration factor and the adherent materials, were all considered and their effectiveness evaluated.

6.2. Bolt-bonded hybrid joints

Balanced single-lap bonded and bolt-bonded hybrid joints with flexible adhesives were studied by Hoang-Ngoc and Paroissien [202] using the FEA. Flexible adhesives were modeled using hyperelastic Mooney-Rivlin potentials. Numerical analyses of bolt-bonded hybrid joints showed their fatigue life is longer than corresponding bolted joints. Kelly [203] investigated Quasi-static strength and fatigue life of bolt-bonded hybrid composite SLJs. A 3D FEA of the hybrid joint was carried out using the ABAQUS code with the model including the effects of large-deformations, bolt–hole contact and non-linear adhesive material properties. Fig. 16 shows the finite element model of the bolt-bonded hybrid SLJ. Three distinct stages in the fatigue life of the hybrid joints were observed where the adhesive, the bolt and their combination were all contributing to the load transfer.

A specimen was developed by Carlberger and Stigh [204] for real-like low velocity impact testing of bi-material joint configurations. The FEA showed good agreement with experiments in

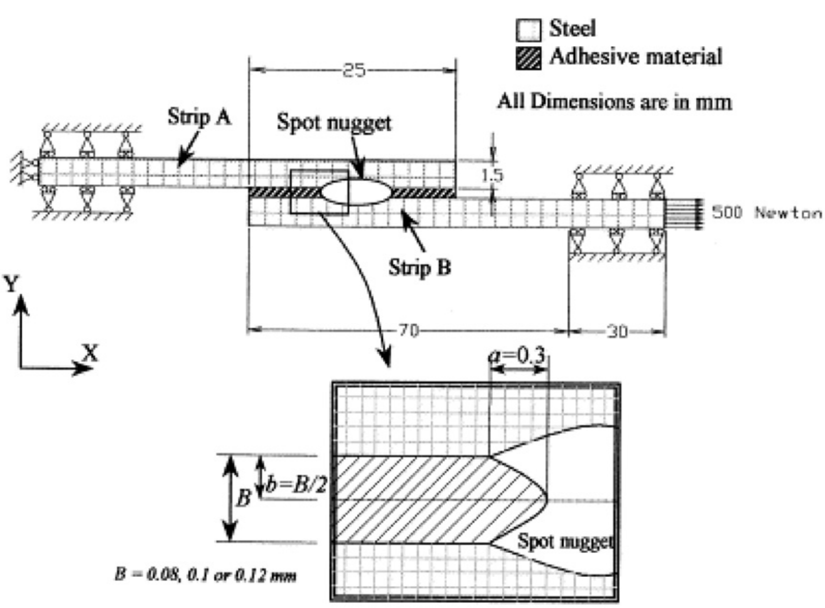

Fig. 15. Finite-element model for weld-bonded joint [199].

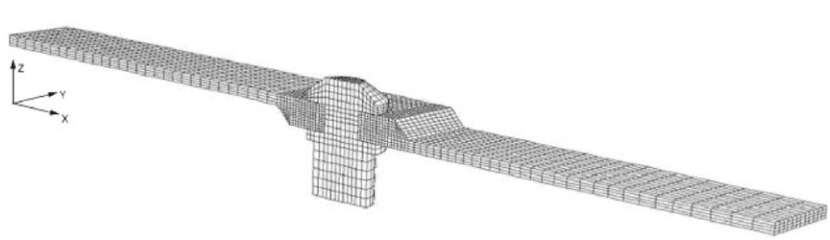

Fig. 16. Finite element model of the bolt-bonded hybrid SLJ [203].

impact energy and overall deformation mode. The authors concluded that a threshold value for the fracture energy of the adhesive seems to exist. Beneath this value, adhesive and discrete fastener work together increasing the impact energy capacity. Above this value the discrete fastener has a negative effect, and may be regarded as a stress concentration.

6.3. Clinch-bonded hybrid joints

A detailed series of tests and FEA were conducted by Grant et al. [205] for Clinch-bonded hybrid joints. The experimental results were compared with spotwelded joints and adhesively bonded double-lap joints. It was concluded that this joint fails because of large plastic deformation in the adherend. Using FEA, Pirondi and Moroni [206] simulated the failure behavior of clinch-bonded and rivet-bonded hybrid joints. The analyses were conducted using Arbitrary Lagrangian–Eulerian (ALE) adaptive meshing to avoid excessive element distortion and mass scaling to increase the minimum time increment in explicit analyses. The authors concluded that different damage models, tuned with experiments performed on simple joints (riveted, clinched or adhesively bonded), can be combined in a unique model to simulate effectively the failure behavior of hybrid joints. By means of 3D ANSYS FEA, the influence of Young's modulus and Poisson's ratio of the structural adhesives on the natural frequencies, natural frequency ratios, and mode shapes of the single-lap clinch-bonded hybrid joints was deduced by He et al. [207].

6.4. Rivet-bonded hybrid joints

A 3D FEA of the riveting process was simulated by Atre and Johnson [208] to determine the effects of interference and adhesive on the induced stresses. Both implicit and explicit finite element techniques were utilized to model the process. The analysis with adhesive showed an increase in the residual hoop stress for the majority of the cases in comparison to the results without adhesive.

Using the commercially available ANSYS FEA program, He et al. [209] studied the torsional free vibration behavior of SLJ encastre hybrid SPR-bonded beams. The mode shapes showed that there are different deformations in the jointed section of the odd and even modes. These different deformations may result different dynamic response and different stress distributions. Recent work by the same authors investigated in detail the free transverse vibration characteristics of single-lap SPR-bonded hybrid joints [210]. The FEA results showed that the stiffer adhesive is likely to suffer fatigue failure and debonding more often than the softer adhesive. These deformations may result in relatively high stresses in the adhesive layers and initiate local cracking and delamination failures.

7. Summary

Due to its low manufacturing cost, low stress concentration and ease of maintenance, adhesive bonding is now one of the most commonly and widely used joining systems in various industrial applications. Adequate understanding of the behavior of adhesively bonded joints is necessary to ensure efficiency, safety and reliability of such joints. However, accurate and reliable modeling of adhesively bonded joints is still a difficult task as the mechanical behavior of these joints is not only influenced by the geometric characteristics of the joint but also by different factors and their combinations.

The information that can be obtained from the FEA of adhesively bonded joints includes: differences in the basic mechanical properties, hygrothermal behavior, occurrence of high stress gradients in certain regions of the joints. An accurate FEA model of adhesive bonded joint must be able to predict failure in the adhesive and at the adhesive–adherend interfaces, and must also account for full non-linear material behavior.

It is necessary to address the performance of specific adhesive–adherends combinations and to combine environmental and fatigue studies of adhesively bonded joints. It is also very important to validate the predicted dynamic behavior of adhesive bonding structures from FEA against experimental test results. Little work in these areas has been undertaken.

In this paper the research and progress in FEA of adhesively bonded joints are critically reviewed and current trends in the application of FEA are mentioned. It is concluded that the FEA of adhesively bonded joints will help future applications of adhesive bonding by allowing different parameters to be selected to give as large a process window as possible for joint manufacture. This will allow many tests to be simulated that would currently take too long to perform or be prohibitively expensive in practice, such as modifications to geometry or material properties.

The references presented in this paper are by no means complete but they give a comprehensive representation of different finite element applications on the subjects. The main goal of the paper is to review recent progress in FEA of adhesively bonded joints and to provide a basis for further research.

References

[1] He X. Int J Adv Manuf Technol 2010;48:607.
[2] He X, Pearson I, Young K. J Mater Process Technol 2008;199(1–3):27.
[3] Adams RD, Comyn J, Wake WC. Structural adhesive joints in engineering. London: Chapman and Hall; 1998.
[4] Kinloch AJ. Adhesion and adhesives. London: Chapman and Hall; 1987.
[5] Mays GC, Hutchinson AR. Adhesives in civil engineering. Cambridge University Press; 1992.
[6] Speth DR, Yang Y, Ritter GW. Int J Adhes Adhes 2010;30(2):55.
[7] Marshall SJ, Bayne SC, Baier R, Tomsia AP, Marshall GW. Dental Mater 2010;26(2):e11.
[8] Gegner J. Materialwissenschaft und Werkstofftechnik 2008;39(1):33. In German.
[9] Kwakernaak A, Hofsiede JCJ. SAMPE J 2008;44(5):6.
[10] Volkersen O. Luftfahrtforschung 1938;15:41.
[11] Goland M, Reissner E. J Appl Mech 1944;11:A17.
[12] Cornell RW. J Appl Mech 1953;20:355.
[13] Hart-Smith LJ. CR-112235, NASA Langley Research Center; 1973.
[14] Hart-Smith LJ. CR-112237, NASA Langley Research Center; 1973.
[15] Hart-Smith LJ. In: Kinloch AJ, editor. Developments in adhesives-2. London: Applied Science Publishers; 1981.
[16] He X. PhD dissertation, UK: Univ. of Manchester; 2003.
[17] Adams RD, Peppiatt NA. J Strain Anal 1974;9(3):185.
[18] Adams RD, Peppiatt NA. J Adhes 1977;9(1):1.
[19] Adams RD, Coppendale J, Peppiatt NA. J Strain Anal Eng Des 1978;13(1):1.
[20] Adams RD, Peppiatt NA, Coppendale J. IPC Sci Technol Press 1978:64–78.
[21] Crocombe AD, Adams RD. J Adhes 1982;13(3–4):241.
[22] Adams RD, Harris JA. Org Coat Appl Polym Sci Proc 1982;47:243.
[23] Adams RD, Crocombe AD, Harris JA. Adhesion (Barking, England); 1983. p. 39–58.
[24] Harris JA, Adams RD. Int J Adhes Adhes 1984;4(2):65.
[25] Harris JA, Adams RD. Plast Rubber Inst 1984:1–17.
[26] Adams RD. Institution of Mechanical Engineers Conference Publications; 1986. p. 17–24.
[27] Adams RD, Harris JA. Int J Adhes Adhes 1987;7(2):69.
[28] Mackerle J. Model Simulat Mater Sci Eng 1997;5(2):159.
[29] Mackerle J. Model Simulat Mater Sci Eng 2002;10(6):637.
[30] Baldan A. J Mater Sci 2004;39(1):1.
[31] Baldan A. J Mater Sci 2004;39(15):4729.
[32] Banea MD, da Silva LFM. P I Mech Eng L-J Mater 2009;223(1):1.
[33] Apalak MK, Ekici R, Yildirim MJ. Sci Ind Res 2008;67(10):797.
[34] Apalak MK, Ekici R, Yildirim M. J Adhes 2007;83(11):957.
[35] Apalak MK, Gunes R. Mater Des 2007;28(5):1597.
[36] Apalak MKJ. Adhes Sci Technol 2006;20(9):1019.
[37] Apalak MK, Gunes R, Eroglu S. Int J Adhes Adhes 2007;27(1):26.
[38] da Silva LFM, Öchsner A. Modeling of adhesive bonded joints. Berlin: Springer; 2008.
[39] da Silva LFM, Öchsner A. Int J Adhes Adhes 2010;30(5):255.
[40] da Silva LFM, Öchsner AJ. Adhes 2010;86(5–6):467.

[41] da Silva LFM, Rodrigues TNSS, Figueiredo MAV, de Moura MFSF, Chousal JAG. J Adhes 2006;82(11):1091.
[42] da Silva LFM, Adams RD, Gibbs M. Int J Adhes Adhes 2010;24(1):69.
[43] Marques EAS, da Silva LFM. J Adhes 2008;84(11):917.
[44] Pinto AMG, Campilho RDSG, de Moura MFSF, Mendes IR. Int J Adhes Adhes 2010;30(5):329.
[45] de Moura MFSF, Daniaud R, Magalhães AG. Int J Adhes Adhes 2006; 26(6):464.
[46] Ichikawa K, Shin Y, Sawa T, Iwamoto T. Trans Jpn Soc Mech Eng Ser A 2009; 75(751):279.
[47] Sawa T, Ichikawa K, Shin Y, Kobayashi T. Int J Adhes Adhes 2010;30(5): 298.
[48] Ichikawa K, Shin Y, Sawa T. Trans Jpn Soc Mech Eng Ser A 2009;75(759): 1562.
[49] He D, Sawa T, Iwamoto T, Hirayama Y. Int J Adhes Adhes 2010;30(6):387.
[50] Ichikawa K, Shin Y, Sawa T. Int J Adhes Adhes 2007;27(8):464.
[51] Shahin K, Taheri F. Compos Struct 2009;90(2):130.
[52] Shahin K, Taheri F. J Adhes Sci Technol 2009;23(10–11):1531.
[53] Shahin K, Kember G, Taheri F. Mech Adv Mater Struct 2008;15(2):88.
[54] Shahin K, Taheri F. Compos Struct 2007;81(4):511.
[55] Hosseinzadeh R, Shahin K, Taheri F. J Adhes Sci Technol 2007;21(16):1613.
[56] Crocombe AD. J Adhes 2008;84(3):212.
[57] Hafiz TA, Wahab MMA, Crocombe AD, Smith PA. Eng Fract Mech 2010;77(17):3434.
[58] Palaniappan J, Wang H, Ogin SL, Thorne AM, Reed GT, Crocombe AD, et al. Compos Sci Technol 2007;67(13):2847.
[59] Palaniappan J, Ogin SL, Thorne AM, Reed GT, Crocombe AD, Capell TF, et al. Compos Sci Technol 2008;68(12):2410.
[60] Jumbo FS, Ashcroft IA, Crocombe AD, Wahab MMA. Int J Adhes Adhes 2010;30(7):523.
[61] Zheng X-L, Zhao M-R, You M, Li Z, Jin H-J. Mater Sci Technol 2009;17(2):16. [In Chinese].
[62] You M, Li Z, Zhao M-R, Guo B, Yan J-L. Trans China Weld Inst 2009;30(11):13. [In Chinese].
[63] Kong F-R, You M, Zheng X-L. J Adhes 2008;84(2):105.
[64] Yan Z-M, You M, Yi X-S, Zheng X-L, Li Z. Int J Adhes Adhes 2007;27(8):687.
[65] Kong F-R, You M, Zheng X-L, Yu H-Z. Int J Adhes Adhes 2007;27(4):298.
[66] Zhao B, Lu Z-H. Mech Adv Mater Struct 2009;16(2):130.
[67] He X, Oyadiji SO. Proceedings of ESDA2004, Manchester; 2004. p. 397.
[68] He X, Oyadiji SO. Proceedings of ESDA2004, Manchester; 2004. p. 405.
[69] Haghani R, Al-Emrani M, Kliger RJ. Compos Mater 2010;44(3):287.
[70] Fessel G, Broughton JG, Fellows NA, Durodola JF, Hutchinson AR. Int J Adhes Adhes 2007;27(7):574.
[71] Zhao X, Adams RD, da Silva LFM. Int J Adhes Adhes 2010;30(2):63.
[72] Grant LDR, Adams RD, da Silva LFM. Int J Adhes Adhes 2009;29(4):405.
[73] Díaz J, Romera L, Hernández S, Baldomir A. Int J Adhes Adhes 2010;30(3):178.
[74] You M, Yan Z-M, Zheng X-L, Yu H-Z, Li Z. Int J Adhes Adhes 2008;28(1–2):71.
[75] You M, Li Z, Zheng X-L, Yu S, Li G-Y, Sun D-X. Int J Adhes Adhes 2009;29(3):280.
[76] Pereira AM, Ferreira JM, Antunes FV, Bártolo PJ. J Mater Process Technol 2010;210(4):610.
[77] Rudawska A. Int J Adhes Adhes 2010;30(7):574.
[78] Kumar S, Pandey PC. J Adhes Sci Technol 2010;24(7):1251.
[79] Llopart PL, Tserpes KI, Labeas GN. Compos Struct 2010;92(7):1673.
[80] Ruiz PD, Jumbo F, Seaton A, Huntley JM, Ashcroft IA, Swallowe GM. J Strain Anal Eng Des 2006;41(8):583.
[81] Jumbo F, Ruiz PD, Yu Y, Swallowe GM, Ashcroft IA, Huntley JM. Strain 2007;43(4):319.
[82] You M, Yan Z-M, Zheng X-L, Yu H-Z, Li Z. Int J Adhes Adhes 2007;27(8):696.
[83] Ascione F, Mancusi G. Mech Adv Mater Struct 2010;17(2):85.
[84] Chataigner S, Caron J-F, Diaz A, Aubagnac C, Benzarti K. Int J Adhes Adhes 2010;30(1):10.
[85] Apalak ZG. J Thermoplastic Compos Mater 2010;23(1):35.
[86] Chaves FJP, da Silva LFM, De Castro PMST. Proc Inst Mech Eng Part L: J Mater: Des Appl 2008;222(3):159.
[87] Grant LDR, Adams RD, da Silva LFM. J Adhes Sci Technol 2009;23(2):317.
[88] Hosseinzadeh R, Cheraghi N, Taheri F. J Strain Anal Eng Des 2006;41(6):443.
[89] Cognard JY, Devaux H, Sohier L. Int J Adhes Adhes 2010;30(8):706.
[90] Vallée T, Tannert T, Murcia-Delso J, Quinn DJ. Int J Adhes Adhes 2010;30(7): 583.
[91] Nisar JA, Hashim SA. Int J Adhes Adhes 2010;30(8):763.
[92] Lavernhe P, Estivalèzes E, Lachaud F, Lodter C, Piquet R. Int J Adhes Adhes 2010;30(1):21.
[93] Koguchi H, Meo N. Trans Jpn Soc Mech Eng, Ser A 2006;72(11):1598. [In Japanese].
[94] Koguchi H, Taniguchi T. Trans Jpn Soc Mech Eng, Ser A 2008;74(6):864. [In Japanese].
[95] Koguchi H, Konno N. Trans Jpn Soc Mech Eng, Ser A 2009;75(757):1148. [In Japanese].
[96] Kilic B, Madenci E, Ambur DR. Eng Fract Mech 2006;73(11):1472.
[97] Kaneko K, Narahashi K. Trans Jpn Soc Mech Eng, Ser A 2007;73(2):201. [In Japanese].
[98] Iwasa M. JSME Int J Ser A: Solid Mech Mater Eng 2006;48(4):256.
[99] Shokrieh MM, Lessard LB, Golubovic A. Iran Polym J (Engl Ed) 2007;16(5):291.
[100] Van Tooren MJL, Gleich DM, Beukers A. J Adhes Sci Technol 2004;18(4):395.
[101] Goglio L, Rossetto M. Int J Adhes Adhes 2010;30(5):313.
[102] Cognard JY. Comput Struct 2008;86(17–18):1704.
[103] Sawa T, Akita Y, Iwamoto T. J Adhes Sci Technol 2009;23(2):195.
[104] Hadavinia H, Kawashita L, Kinloch AJ, Moore DR, Williams JG. Eng Fract Mech 2006;73(16):2324.
[105] Kim H. Compos Sci Technol 2006;66(14):2456.
[106] Ueda M, Shishido N, Ikeda T, Miyazaki N. Trans Jpn Soc Mech Eng, Ser A 2009;75(759):1516. [In Japanese].
[107] Ferraris M, Ventrella A, Salvo M, Avalle M, Pavia F, Martin E. Compos Part B: Eng 2010;41(2):182.
[108] Ascione F, Mancusi G. Mech Adv Mater Struct 2010;17(2):157.
[109] Iwamoto T, Nagai T, Sawa T, Kuramoto H, Uesugi N. Trans Jpn Soc Mech Eng, Ser A 2009;75(758):1402. [In Japanese].
[110] Panigrahi SK, Pradhan B. J Adhes Sci Technol 2007;21(5–6):379.
[111] Panigrahi SK. Appl Compos Mater 2009;16(4):211.
[112] Kahraman R, Sunar M, Yilbas B. J Mater Process Technol 2008;205(1–3):183.
[113] Wang J, Zhang C. Int J Solids Struct 2009;46(25–26):4409.
[114] Lu L, Zhao HY, Cai ZP, Wang PC, Fickes J. Sci Technol Weld Join 2008;13(5): 479.
[115] Esmaeel RA, Taheri F. J Adhes Sci Technol 2009;23(13–14):1827.
[116] Choupani N. Eng Fract Mech 2008;75(15):4363.
[117] Shahin K, Taheri F. Int J Solids Struct 2008;45(25–26):6284.
[118] Campilho RDSG, de Moura MFSF, Pinto AMG, Morais JJL, Domingues JJMS. Compos Part B: Eng 2009;40(2):149.
[119] Campilho RDSG, de Moura MFSF, Domingues JJMS. Int J Adhes Adhes 2009;29(2):195.
[120] Campilho RDSG, de Moura MFSF, Domingues JJMS, Morais JJL. J Adhes Sci Technol 2008;22(13):1565.
[121] Campilho RDSG, de Moura MFSF, Domingues JJMS. Int J Solids Struct 2008;45(5):1497.
[122] Campilho RDSG, de Moura MFSF, Domingues JJMS. J Adhes Sci Technol 2007;21(9):855.
[123] Das RR, Pradhan B. Int J Adhes Adhes 2010;30(6):425.
[124] Schmidt Peter, Edlund Ulf. Int J Adhes Adhes 2010;30(8):665.
[125] Ouyang Z-y, Li G-q. Int J Solids Struct 2009;46(5):1205.
[126] Ouyang Z-y, Li G-q. Int J Fract 2009;155(1):19.
[127] Ouyang Z-y, Li G-q. J Appl Mech, Trans ASME 2009;76(5):1.
[128] de Moura MFSF, Campilho RDSG, Gonçalves JPM. Int J Solids Struct 2009;46(6):1589.
[129] de Moura MFSF, Campilho RDSG, Gonçalves JPM. Compos Sci Technol 2008;68(10–11):2224.
[130] Sun C, Thouless MD, Waas AM, Schroeder JA, Zavattieri PD. Int J Fract 2009;156(2):111.
[131] Lee C-J, Lee S-K, Ko D-C, Kim B-M. Trans Korean Soc Mech Eng, Ser A 2009;33(5):474.
[132] Fan C, Jar PYB, Cheng JJR. Eng Fract Mech 2008;75(13):3866.
[133] Martiny Ph, Lani F, Kinloch AJ, Pardoen T. Int J Adhes Adhes 2008;28(4–5):222.
[134] Alfano M, Furgiuele F, Leonardi A, Maletta C, Paulino GH. Key Eng Mater 2007;348–349:13.
[135] Crocombe AD, Hua YX, Loh WK, Wahab MA, Ashcroft IA. Int J Adhes Adhes 2006;26(5):325.
[136] Li Z, You M, Zheng X-L, Zhao M-R, Yan J-L. Chin J Comput Mech 2008;25:86. [In Chinese].
[137] Mubashar A, Ashcroft IA, Critchlow GW, Crocombe AD. J Adhes 2009; 85(10):711.
[138] Liljedahl CDM, Crocombe AD, Wahab MA, Ashcroft IA. J Adhes 2006; 82(11):1061.
[139] Tsai MY, Wu CY, Huang CY, Yang SS. IEEE Trans Adv Packag 2008;31(3):454.
[140] Hua YX, Crocombe AD, Wahab MA, Ashcroft IA. J Adhes 2006;82(2):135.
[141] Hua YX, Crocombe AD, Wahab MA, Ashcroft IA. Int J Adhes Adhes 2008;28(6):302.
[142] Hua YX, Crocombe AD, Wahab MA, Ashcroft IA. J Adhes Sci Technol 2007; 21(2):179.
[143] Aydin MD, Temiz S, Ozel A. J Adhes 2007;83(6):553.
[144] Grant LDR, Adams RD, da Silva LFM. Int J Adhes Adhes 2009;29(5):535.
[145] Zhang Y, Vassilopoulos AP, Keller T. Compos Struct 2010;92(7):1631.
[146] Apalak MK, Gunes R. J Adhes Sci Technol 2006;20(12):1295.
[147] da Silva LFM, Adams RD. J Adhes Sci Technol 2006;20(15):1705.
[148] da Silva LFM, Adams RD. Int J Adhes Adhes 2007;27(3):216.
[149] da Silva LFM, Adams RD. Int J Adhes Adhes 2007;27(5):362.
[150] das Neves PJC, da Silva LFM, Adams RD. J Adhes Sci Technol 2009;23(1):1.
[151] das Neves PJC, da Silva LFM, Adams RD. J Adhes Sci Technol 2009;23(1):35.
[152] Malvade I, Deb A, Biswas P, Kumar A. Comput Mater Sci 2009;44(4):1208.
[153] Jen Y-M, Ko C-W. Int J Fatigue 2010;32(2):330.
[154] Bernasconi A, Beretta S, Moroni F, Pirondi A. J Adhes 2010;86(5–6):480.
[155] Pereira AM, Ferreira JM, Antunes FV, Bártolo PJ. Int J Adhes Adhes 2009;29(6):633.
[156] Quaresimin M, Ricotta M. Compos Sci Technol 2006;66(5):647.
[157] Bachir Bouiadjra B, Fekirini H, Belhouari M, Boutabout B, Serier B. Comput Mater Sci 2007;40(1):20.
[158] Wang J, Rider AN, Heller M, Kaye R. Int J Adhes Adhes 2005;25(5):410.
[159] Ferreira JM, Silva H, Costa JD, Richardson M. Compos Part B 2005;36(1):1.
[160] Datla NV, Papini M, Schroeder JA, Spelt JK. Int J Adhes Adhes 2010; 30(6):439.
[161] Graner Solana A, Crocombe AD, Ashcroft IA. Int J Adhes Adhes 2010; 30(1):36.

[162] Pirondi A, Moroni F. J Adhes 2010;86(5–6):501.
[163] Fessel G, Broughton JG, Fellows NA, Durodola JF, Hutchinson AR. Fatigue Fract Eng Mater Struct 2009;32(9):704.
[164] Marannano GV, Mistretta L, Cirello A, Pasta S. Eng Fract Mech 2008;75(18):5122.
[165] Ishii K, Imanaka M, Nakayama H. J Adhes Sci Technol 2007;21(2):153.
[166] Shenoy V, Ashcroft IA, Critchlow GW, Crocombe AD, Wahab MMA. Int J Adhes Adhes 2009;29(4):361.
[167] Shenoy V, Ashcroft IA, Critchlow GW, Crocombe AD. Int J Fatigue 2010;32(8):1278.
[168] Wahab MMA, Hilmy I, Ashcroft IA, Crocombe AD. J Adhes Sci Technol 2010;24(2):325.
[169] Keller T, Schollmayer M. Compos Struct 2009;87(3):232.
[170] Hosseini-Toudeshky H, Saber M, Mohammadi B. Finite Elem Anal Des 2009;45(2):94.
[171] Khoramishad H, Crocombe AD, Katnam KB, Ashcroft IA. Int J Adhes Adhes 2010;30(6):513.
[172] Ghoneam SM, Hamada AA, EL-Elamy MI. Diffusion Defect Data Pt. B: Solid State Phenom 2009;147–149:663.
[173] Apalak MK, Yildirim M. J Adhes Sci Technol 2007;21(3–4):267.
[174] Apalak MK, Ekici R, Yildirim M, Erkaya S. J Adhes Sci Technol 2009; 23(2):339.
[175] Pandurangan P, Buckner GD. Exp Mech 2006;46(5):601.
[176] He X. Adv Mater Res 2010;97–101:3920.
[177] Kaya A, Tekelioglu MS, Findik F. Mater Lett 2004;58(27–28):3451.
[178] Bartoli I, Marzani A, Lanza di Scalea F, Viola Erasmo. J Sound Vib 2006; 295(3–5):685.
[179] Kim DI, Jung SC, Lee JE, Chang SH. Compos Struct 2006;75(1–4):408.
[180] He X, Oyadiji SO. J Mater Process Technol 2001;119:366.
[181] Apalak MK, Ekici R, Yildirim M. J Adhes Sci Technol 2006;20(13):1507.
[182] Apalak MK, Yildirim M. J Thermoplastic Compos Mater 2009;22(2):183.
[183] He X. Key Eng Mater 2009;413–414:733.
[184] Apalak MK, Yildirim M. Polym Polym Compos 2007;15(6):489.
[185] Gunes R, Apalak MK, Yildirim M. Int J Mech Sci 2007;49(4):479.
[186] Gunes R, Apalak MK, Yildirim M, Ozkes I. Compos Struct 2010;92(1):1.
[187] Carlberger T, Stigh U. Eng Fract Mech 2007;74(14):2247.
[188] Sawa T, Nagai T, Iwamoto T, Kuramoto H. Proc ASME IMECE 2008;15:55.
[189] Iwamoto T, Nagai T, Sawa T, Kuramoto H, Uesugi N. Trans Jpn Soc Mech Eng, Ser A 2009;75(757):1141. [in Japanese].
[190] Park H, Kim H. Int J Impact Eng 2010;37(2):177.
[191] Silberschmidt VV, Casas-Rodriguez JP, Ashcroft IA. Key Eng Mater 2009;399:71.
[192] Challita G, Othman R. Int J Adhes Adhes 2010;30(4):236.
[193] Sawa T, Ichikawa K. Proc ASME DE 2005;118B(2):819.
[194] Vaidya UK, Gautam ARS, Hosur M, Dutta P. Int J Adhes Adhes 2006; 26(3):184.
[195] Kim H, Kayir T, Mousseau SL. J Compos Mater 2005;39(22):2039.
[196] Yin Y, Chen J-J, Tu S-T. Mech Time-Depend Mater 2005;9(1):91.
[197] Zhao B, Yue P. Chin J Appl Mech 2008;25(1):24. [In Chinese].
[198] Darwish SM, Al-Samhan A. J Mater Process Technol 2004;153–154(1–3):971.
[199] Darwish SM, Al-Samhan A. Int J Adhes Adhes 2004;24(5):367.
[200] Darwish SM. Int J Adhes Adhes 2004;24(4):347.
[201] Darwish SM, Al-Samhan A. J Mater Process Technol 2004;147(1):51.
[202] Hoang-Ngoc C-T, Paroissien E. Int J Adhes Adhes 2010;30(3):117.
[203] Kelly G. Compos Struct 2006;72(1):119.
[204] Carlberger T, Stigh U. Thin Wall Struct 2010;48(8):609.
[205] Grant LDR, Adams RD, da Silva LFM. J Adhes Sci Technol 2009;23(12):1673.
[206] Pirondi A, Moroni F. J Adhes Sci Technol 2009;23(10–11):1547.
[207] He X, Gao S, Zhang W. Proc ICMTMA2010 2010:1027.
[208] Atre A, Johnson WS. J Aircraft 2007;44(2):353.
[209] He X, Dong B, Zhu X. AIP Conf Proc 2009;1233:678.
[210] He X, Zhu X, Dong B. Proc MIMT2010 2010:389.